

AD-A085 867

ATOMIC WEAPONS RESEARCH ESTABLISHMENT ALDERMASTON (EN--ETC F/6 17/9
THE CALCULATION OF RADAR CROSS-SECTIONS, (U)

APR 80 R PIZER

AWRE-0-44/79

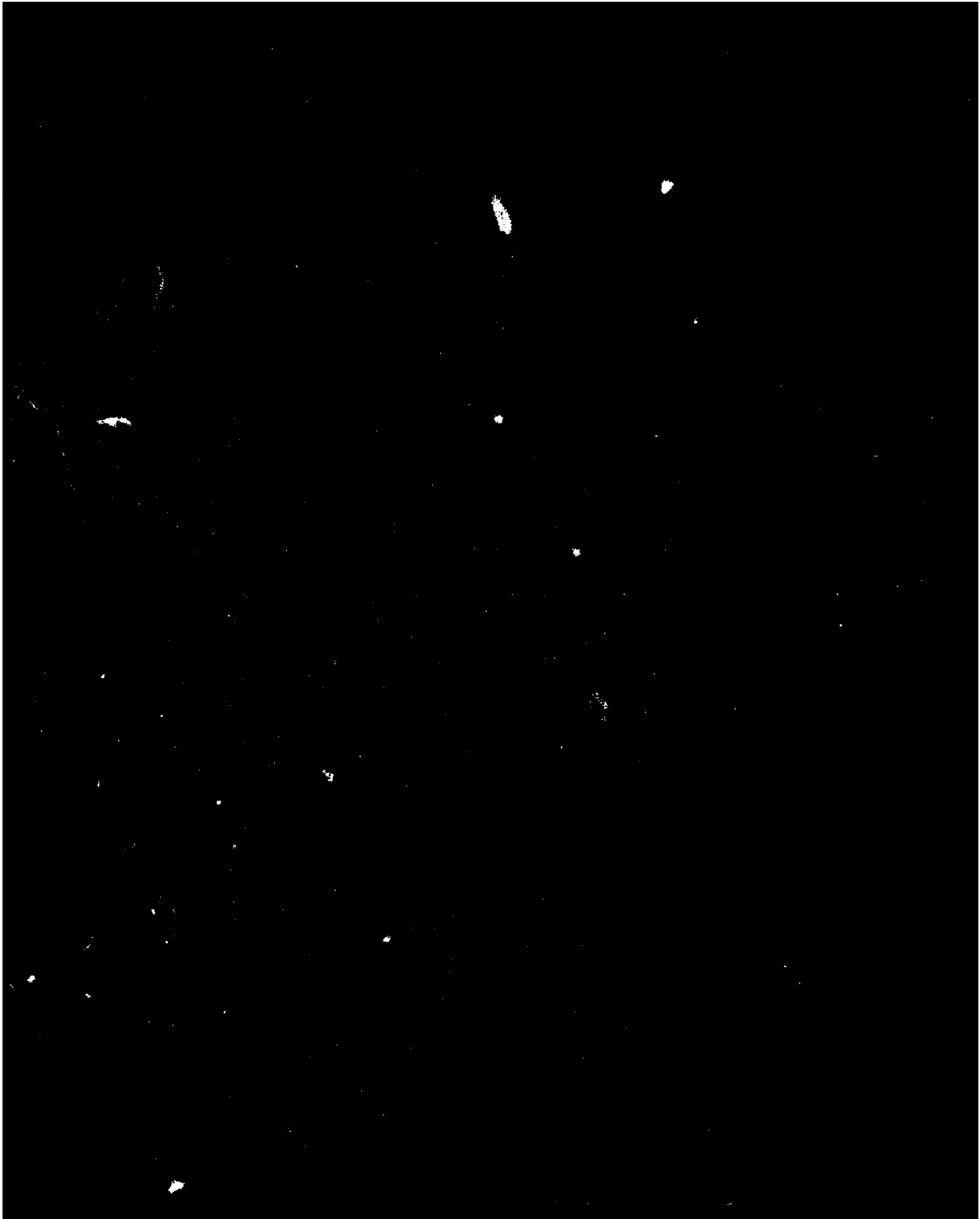
DRIC-BR-73529

NL

UNCLASSIFIED

[OP]
AD
AUG 80

END
DATE
FILMED
8-80
DTIC





11 Apr 80

Procurement Executive - Ministry of Defence

18 DRIC

19 BR-73529

AWRE, Aldermaston

14 AWRE-0-44/79

AWRE REPORT NO. 044/79

6 The Calculation of Radar Cross-Sections

10 R Pizer

12 95

Approved for issue by

A H Armstrong, Senior Superintendent

DTIC ELECTE JUN 12 1980

B

046650 Jue

CONTENTS

	<u>Page</u>
SUMMARY	4
1. INTRODUCTION	4
2. THE DERIVATION OF THE CHAOS EQUATIONS	5
2.1 Maxwell's equations in the frequency domain	5
2.2 Homogeneous materials assumption	6
2.3 Helmholtz's equations for potentials	7
2.4 Solution of Helmholtz's equations for conductors	7
2.5 Boundary conditions	8
2.6 Thin wire approximation	8
2.7 Currents due to plane wave excitation	9
2.8 Equation for the currents	10
3. NUMERICAL REPRESENTATION OF THE PHYSICS	11
3.1 Representation of the currents	11
3.2 Choice of weighting function	11
3.3 Form of impedance matrix	12
3.4 Matrix factorization	14
3.5 Calculation of electric fields	15
3.6 Radar cross-sections	16
3.7 Numerical evaluation of impedance matrix elements	16
3.8 Numerical evaluation of the voltage vector	19
4. JUNCTIONS OF WIRES	19
4.1 Chao and Strait's method	20
4.2 Sayre's method	21
4.3 50/50 method	22
4.4 Other methods	22
4.5 Effects on impedance matrix elements	23
5. WIRE MESH MODELLING OF SOLID SURFACES	26
6. TREATMENT OF MATERIALS WHICH ARE NOT PERFECTLY CONDUCTING	28
6.1 Types of current	28
6.2 Impedance of wire	29
6.3 Form of matrix of contributions due to finite conductivity	32
6.4 Lumped loads	32
7. SYMMETRIES IN GEOMETRICAL STRUCTURE	33
7.1 Rotational symmetry	34
7.2 Left-right symmetry	39
7.3 Two planes of mirror symmetry	41

CONTENTS (CONT.)

	<u>Page</u>
8. SPARSE MATRIX APPROXIMATION	43
9. COMPLEX FREQUENCY VERSION OF CHAOS	44
FIGURES 1 - 11	47
APPENDIX A: ACCURACY	58
FIGURE A1	66
APPENDIX B: CONVENTIONS USED IN CHAOS	67
FIGURES B1 - B4	81
APPENDIX C: LIST OF SYMBOLS	85
REFERENCES	89

ACCESSION for		
NTIS	White Section	<input checked="" type="checkbox"/>
DDC	Buff Section	<input type="checkbox"/>
UNANNOUNCED		<input type="checkbox"/>
JUSTIFICATION _____		
BY _____		
DISTRIBUTION/AVAILABILITY CODES		
Dist.	AVAIL.	and/or SPECIAL
A		

SUMMARY

This report provides a detailed description of the methods used in the computer program CHAOS for calculating radar cross-sections.

1. INTRODUCTION

The object of this report is to provide a detailed description of the methods used in the CHAOS computer program for calculating radar cross-sections. The program is written in FORTRAN.

The various physical approximations are described, ~~in section 2~~. These help to simplify Maxwell's equations. At first sight these would appear to limit the scattering bodies to open wire structures; however, extensions to surfaces both open and closed follow by further approximation (~~section 5~~). The numerical methods used to solve these equations are described, ~~in section 3~~.

The problem of wire junctions is tackled in section 4 while section 6 deals with finite conductivity and shows how lumped loads may be attached to the structure. Some special techniques for dealing with bodies having rotational or left-right symmetries are described in section 7. Sections 8 and 9 briefly describe the sparse matrix approximation and the complex frequency version of CHAOS respectively.

Three appendices are also provided. Appendix A deals with the formulae used to calculate the impedance matrix elements and gives reasons for various restrictions regarding segment length and radius. Appendix B describes the conventions adopted throughout the programme concerning coordinate systems and polarisation. A list of frequently used symbols is given in appendix C.

2. THE DERIVATION OF THE CHAOS EQUATIONS

2.1 Maxwell's equations in the frequency domain

We start from Maxwell's equations. These are:-

Faraday's law of induction:

$$\nabla \wedge \underline{E} = - \frac{\partial \underline{B}}{\partial t}, \quad \dots(1)$$

Gauss' law:

$$\nabla \cdot \underline{D} = \rho, \quad \dots(2)$$

Maxwell's generalisation of Ampère's law:

$$\nabla \wedge \underline{H} = \frac{\partial \underline{D}}{\partial t} + \underline{J}. \quad \dots(3)$$

and finally

$$\nabla \cdot \underline{B} = 0. \quad \dots(4)$$

In these equations the symbols have the following meaning:-

- \underline{E} = complex electric field,
- \underline{D} = complex electric flux,
- \underline{H} = complex magnetic field,
- \underline{B} = complex magnetic flux,
- \underline{J} = complex conduction current,
- ρ = complex electric charge,
- t = time,

and the rationalised system of MKS units has been used. At this point we have the choice of working in the time domain, so that we can deal with an initial pulse which is some arbitrary function of time, or of specifying some particular time behaviour. We choose the latter and assume a time variation of $e^{i\omega t}$ where ω is the frequency of the electromagnetic wave. This is known as working in the frequency domain. Thus, this type of

approach is ideally suited to calculating radar cross-sections for radars of the continuous wave type. For radars which send out short pulses containing components spread over many frequencies, it is necessary to Fourier analyse the pulse and do calculations for all the frequencies in the pulse before combining together to get the scattered field and radar cross-section. Despite the apparent clumsiness of this approach, it appears to be more reliable than working directly in the time domain.

By specifying that all the quantities in Maxwell's equations have a time variation $e^{i\omega t}$, we obtain

$$\begin{array}{l}
 \nabla \wedge \underline{E} = -i\omega \underline{B} \quad \} \\
 \nabla \cdot \underline{D} = \rho \quad \} \\
 \nabla \wedge \underline{H} = i\omega \underline{D} + \underline{J} \quad \} \\
 \nabla \cdot \underline{B} = 0. \quad \}
 \end{array} \quad \dots(5)$$

2.2 Homogeneous materials assumption

There is a relation between the variables \underline{D} and \underline{E} and another relation between the variables \underline{B} and \underline{H} . It is known that for some materials these pairs of variables are linearly related and we have

$$\begin{array}{l}
 \underline{D} = \epsilon \underline{E}, \\
 \underline{B} = \mu \underline{H},
 \end{array}$$

where ϵ and μ are scalars called the dielectric constant and permeability respectively. For homogeneous materials ϵ and μ are independent of position in the body. So equations (5) reduce to

$$\begin{array}{l}
 \nabla \wedge \underline{E} = -i\omega \mu \underline{H} \quad \} \\
 \nabla \cdot \underline{E} = \rho/\epsilon \quad \} \\
 \nabla \wedge \underline{H} = i\omega \epsilon \underline{E} + \underline{J} \quad \} \\
 \nabla \cdot \underline{H} = 0. \quad \}
 \end{array} \quad \dots(6)$$

2.3 Helmholtz's equations for potentials

From the last of equations (6) we have

$$\underline{H} = \frac{1}{\mu} \nabla \wedge \underline{A}, \quad \dots(7)$$

where \underline{A} is the magnetic vector potential. The first of equations (6) may now be integrated to give

$$\underline{E} = -i\omega \underline{A} - \nabla \phi, \quad \dots(8)$$

where ϕ is the electric scalar potential and is, at present, some arbitrary function. By substituting in the remaining two equations we get the Helmholtz equations:-

$$\begin{aligned} \nabla^2 \underline{A} + k^2 \underline{A} &= -\mu \underline{J}, \\ \nabla^2 \phi + k^2 \phi &= -\rho/\epsilon, \end{aligned} \quad \dots(9)$$

where $k^2 = \omega^2 \epsilon \mu$ and we have chosen to impose on ϕ the so called Lorentz condition

$$\nabla \cdot \underline{A} = -i\omega \epsilon \mu \phi. \quad \dots(10)$$

2.4 Solution of Helmholtz's equations for conductors

Now we can formally solve the Helmholtz equations and since for conductors it is known that the current \underline{J} and charge ρ reside on or very close to the surface, the vector equation gives

$$\underline{A}(\underline{r}) = \mu \iint \underline{J}(\underline{r}') \frac{e^{-ikR}}{4\pi R} ds', \quad \dots(11)$$

where R is the distance between the observation point \underline{r} and some point \underline{r}' on the surface of the conductor. The scalar equation gives

$$\phi(\underline{r}) = \frac{1}{\epsilon} \iint \rho(\underline{r}') \frac{e^{-ikR}}{4\pi R} ds'. \quad \dots(12)$$

In both these expressions ds' is an element of area of the surface of the conductor and the integrations are over the whole surface. There is one further equation relating the current \underline{J} and the charge ρ which is the law of conservation of charge obtained by differentiating the third of equations (5)

$$\nabla \cdot \underline{J} = -i\omega\rho. \quad \dots(13)$$

2.5 Boundary conditions

At a boundary between two different materials, the following conditions are observed:-

$$\begin{aligned} (\underline{E}^{(1)} - \underline{E}^{(2)}) \cdot \underline{n} &= 0, \\ \underline{n} \cdot (\underline{D}^{(1)} - \underline{D}^{(2)}) &= \rho_s, \\ \underline{n} \wedge (\underline{H}^{(1)} - \underline{H}^{(2)}) &= \underline{J}_s, \\ \underline{n} \cdot (\underline{B}^{(1)} - \underline{B}^{(2)}) &= 0, \end{aligned} \quad \dots(14)$$

where the superscripts (1) and (2) refer to the fields on either side of the material boundary, and \underline{n} is the unit normal to the surface pointing into region (1). Here ρ_s and \underline{J}_s are electric surface charge and current respectively. Since we are solving for the electric field it is the first two which concern us.

2.6 Thin wire approximation

The integrals in (11) and (12) can be further simplified by assuming that we are dealing with thin wires rather than surfaces. While this may appear to restrict the program to dealing with wire structures only, we shall see in section 5 that surfaces can be modelled by wire meshes and this appears to be the best method available for dealing with arbitrarily shaped surfaces of finite conductivity.

Following from the thin wire assumption, we assume that the circumferential current is negligible and replace the axial surface current and the surface charge by a line current, \underline{I} , flowing along the wire axis and a line charge σ . So we have

$$\underline{I} = 2\pi a \underline{J}, \quad \dots(15)$$

$$\sigma = 2\pi a \rho, \quad \dots(16)$$

where a is the wire radius. This leads to

$$\underline{A}(\underline{r}) = \mu \int_{\text{wire}} \underline{I}(\underline{l}') \frac{e^{-ikR}}{4\pi R} d\underline{l}', \quad \dots(17)$$

$$\phi(\underline{r}) = \frac{1}{\epsilon} \int_{\text{wire}} \sigma(\underline{l}') \frac{e^{-ikR}}{4\pi R} d\underline{l}', \quad \dots(18)$$

$$\sigma(\underline{l}) = \frac{i}{\omega} \nabla \cdot \underline{I}(\underline{l}) = \frac{i}{\omega} \frac{d}{d\underline{l}} \underline{I}(\underline{l}), \quad \dots(19)$$

where \underline{l} is the measure of length along the wire. We only try to satisfy the boundary condition on the axial component of the electric field:-

$$(\underline{E}_{\text{tan}}^{(1)} - \underline{E}_{\text{tan}}^{(2)}) = 0, \quad \dots(20)$$

where the subscript tan denotes the component of the electric field parallel to the wire axis.

2.7 Currents due to plane wave excitation

Let us now assume that the scattering body will be illuminated by a plane electric wave, \underline{E}^i , of known amplitude and polarisation. Then the total electric field may be written

$$\underline{E} = \underline{E}^i + \underline{E}^s, \quad \dots(21)$$

where \underline{E}^s is the unknown electric field scattered from the body. Bearing in mind equations (8), (17) and (18) let us write

$$\underline{E}^s = -i\omega \underline{A}^s - \nabla \phi^s, \quad \dots(22)$$

$$\underline{A}^s(\underline{r}) = \mu \int_{\text{wire}} \underline{I}(\ell') \frac{e^{-ikR}}{4\pi R} d\ell', \quad \dots(23)$$

$$\phi^s(\underline{r}) = \frac{1}{\epsilon} \int_{\text{wire}} \sigma(\ell') \frac{e^{-ikR}}{4\pi R} d\ell'. \quad \dots(24)$$

It will be noticed that the superscript s has been omitted from \underline{I} and σ in equations (23) and (24). This is because a plane wave satisfies Maxwell's equations (6) with $\rho = 0$ and $\underline{J} = \underline{0}$, so that the whole of the current and charge distributions induced on the body's surface by the incident plane wave contribute to the scattered fields as one would expect.

The boundary condition (20) may be written

$$(\underline{E}_{\text{tan}}^i + \underline{E}_{\text{tan}}^s - \underline{E}_{\text{tan}}^{(2)}) = 0. \quad \dots(25)$$

2.8 Equation for the currents

We use equation (25) because this relates the scattered field on the body surface to the incident field \underline{E}^i and the field inside the wire $\underline{E}^{(2)}$. For a perfect conductor $\underline{E}^{(2)}$ is zero while for a wire of finite conductivity, it may be calculated approximately and in section 5 an expression of the form

$$\underline{E}_{\text{tan}}^{(2)} = Z_{\omega} \underline{I} \quad \dots(26)$$

will be derived where Z_{ω} is the known impedance matrix of the wires.

So by substituting equations (19), (22), (23), (24) and (26) into equation (25) we obtain an equation for the currents \underline{I} of the form

$$Z_{\omega} \underline{I} - \underline{E}_{\text{tan}}^i = -i \int_{\text{wires}} \left[\omega \mu \underline{I}(\ell') + \frac{1}{\omega \epsilon} \nabla \left(\frac{d\underline{I}(\ell')}{d\ell'} \right) \right] \frac{e^{-ikR}}{4\pi R} d\ell'. \quad \dots(27)$$

This equation is sometimes referred to as the potential integro-differential equation to distinguish it from other variants such as Pocklington's equation, the magnetic vector potential equation and Hallen's equation.

3. NUMERICAL REPRESENTATION OF THE PHYSICS

3.1 Representation of the currents

We now expand the currents in terms of a finite series of known basis functions with unknown amplitudes. If we were dealing with a single wire, the obvious choice would be a set of whole wire functions like, for instance, a Fourier series expansion. However, we wish to be able to deal with bent wires and arbitrarily shaped wire meshes so it is more useful to divide the wires up into a series of short segments and define a set of functions each of which is non-zero over a few segments only.

We choose triangle functions as used by Chao and Strait [1], Mautz and Harrington [2] and Kuo and Strait [3]. As shown in figure 1(a), each triangle function, T_i , is based on four segments and overlaps its neighbour by two segments. It is of unit height. Thus, we expand the current as

$$\underline{I}(\ell) = \sum_{i=1}^N I_i T_i(\ell), \quad \dots(28)$$

where N is the number of triangle functions needed to cover the wires. In this way a piecewise linear approximation to the currents is obtained as depicted in figure 1(b). The amplitudes I_i are the unknowns which we require to find.

Other commonly used basis functions are step functions, sinusoidal functions and a three term function consisting of constant, sine and cosine terms.

3.2 Choice of weighting function

Since we have chosen a finite number of basis functions T_i ($i = 1, \dots, N$), we need to derive N equations from equation (27) to enable us to solve for the unknown amplitudes I_i . We do this by multiplying equation (27) in turn by N weighting functions and integrating over the wire length. These weighting functions could be the delta function

positioned at the centre of each triangle function and in this way we would satisfy equation (27) exactly at these points. However, the solution could be badly in error away from these points and it has been found better to use the basis functions as weighting functions. In this way we do not satisfy equation (27) exactly anywhere, except by accident, but we minimize the overall error of the solution for the current in the least squares sense. This latter scheme is known as the Galerkin procedure, while the former is called point matching or collocation. There is an added attraction to the Galerkin procedure in that the resulting matrix of impedances is symmetric as will be seen shortly. Thus, only half the matrix need be stored in the computer and the principle of reciprocity is automatically satisfied. This is not the case for any other set of weighting functions.

3.3 Form of impedance matrix

By substituting (28) into (27) and carrying out the Galerkin procedure we arrive at the set of equations

$$\sum_{i=1}^N Z_{ji} I_i = V_j, \quad j = 1 \dots N, \quad \dots(29)$$

where the impedance matrix is given by

$$\begin{aligned} Z_{ji} = & \int_{\text{wires}} d\ell Z_{\omega i} T_j(\ell) \cdot T_i(\ell) + i\omega\mu \int_{\text{wires}} d\ell \int_{\text{wires}} d\ell' T_j(\ell) \cdot T_i(\ell') \frac{e^{-ikR}}{4\pi R} \\ & + \frac{i}{\omega\epsilon} \int_{\text{wires}} d\ell T_j(\ell) \cdot \nabla \int_{\text{wires}} d\ell' \frac{dT_i(\ell')}{d\ell'} \frac{e^{-ikR}}{4\pi R} \quad \dots(30) \end{aligned}$$

and the excitation voltages are given by

$$V_j = \int_{\text{wires}} d\ell T_j(\ell) \cdot \underline{E}_{\text{tan}}^i \quad \dots(31)$$

From the form of the last term in equation (30) it appears that Z_{ji} is not symmetric. However, we can manipulate the last term to obtain

$$\begin{aligned}
& \frac{i}{\omega\epsilon} \int_{\text{wires}} d\ell T_j(\ell) \cdot \nabla \int_{\text{wires}} d\ell' \frac{dT_i(\ell')}{d\ell'} \frac{e^{-ikR}}{4\pi R} \\
&= \frac{i}{\omega\epsilon} \int_{\text{wires}} d\ell T_j(\ell) \frac{d}{d\ell} \int_{\text{wires}} d\ell' \frac{dT_i(\ell')}{d\ell'} \frac{e^{-ikR}}{4\pi R}, \\
&= \frac{i}{\omega\epsilon} \left[T_j(\ell) \int_{\text{wires}} d\ell' \frac{dT_i(\ell')}{d\ell'} \frac{e^{-ikR}}{4\pi R} \right]_{\ell=\ell_0}^{\ell=\ell_N} - \frac{i}{\omega\epsilon} \int_{\text{wires}} d\ell \frac{d}{d\ell} T_j(\ell) \int_{\text{wires}} d\ell' \frac{dT_i(\ell')}{d\ell'} \frac{e^{-ikR}}{4\pi R}.
\end{aligned}$$

Now the first term is zero because the currents at the free ends of the wires are assumed to be zero. Thus, Z_{ji} can be written

$$\begin{aligned}
Z_{ji} &= \int_{\text{wires}} d\ell Z_{\omega i-j} T_j(\ell) \cdot T_i(\ell) \dots (32) \\
&+ i \int_{\text{wires}} d\ell \int_{\text{wires}} d\ell' \left[\omega \mu T_j(\ell) \cdot T_i(\ell') - \frac{1}{\omega\epsilon} \frac{d}{d\ell} T_j(\ell) \frac{d}{d\ell'} T_i(\ell') \right] \frac{e^{-ikR}}{4\pi R},
\end{aligned}$$

which is symmetric in i and j which means that the principle of reciprocity is automatically satisfied. At first sight it may appear that equation (32) is only valid for a set of unconnected wires with both ends free. However, once the method of joining wires together is described (in section 4) it will become clear that (32) holds for any wire structure.

It is perhaps worth pointing out that if we were using a surface patch approximation rather than the thin wire approximation, the impedance matrix analogous to that given by equation (30) would be unsymmetric even if Galerkin's technique were used. It is not possible to devise an equation analogous to equation (32) because the current at the edge of a patch is not necessarily zero. Thus, to get a symmetric matrix one must work this in from the start by using the principle of reciprocity. This is the approach adopted by Richmond [4] in his thin wire treatment.

In CHAOS the voltages given by equation (31) are for plane wave excitation. It would not be difficult to modify this equation to cope with a point source, as is seen in antenna problems, so that radiation patterns could be calculated rather than radar cross-sections. However, this has not been done.

3.4 Matrix factorization

Equation (29) for the unknown current amplitudes is solved using the Harwell matrix factorization routine MA29 [5] modified for complex elements. The method is due to Fletcher [6] and the factorization takes the form

$$Z = LDL^T, \quad \dots(33)$$

where L is lower triangular and D is block diagonal, the blocks not exceeding 2×2 in size. As a check on the reliability of the factorization the ratio of the maximum and minimum elements of D is examined. For a 2×2 block in D the square root of the determinant of the block is used. It has been found that if this ratio exceeds 20000 when using a 32 bit computer word length, then the factorization may be unreliable. The matrix Z should be properly scaled and this is usually done automatically by the CHAOS program.

In section 4 the various different wire junction treatments are discussed. Some of these give rise to unsymmetric matrices. For these cases the Harwell routine MA23 [7] is used to factorize the matrix as

$$Z = L.U, \quad \dots(34)$$

where L is lower triangular and U is upper triangular. The reliability of this factorization is checked by examining the ratio of maximum to minimum elements of the diagonal of U. If this exceeds 20000 using a 32 bit computer word length, then the factorization may be unreliable. Again the matrix Z should be properly scaled.

In those cases where the ratio exceeds the value 20000, the calculation is immediately terminated and nothing can be done to get answers, except by modifying the computer program. This latter is not advised.

Once the current amplitudes I_i of the expansion (28) are known, we can find the charge distribution from equation (19) and the scattered electric fields at any point in space from equations (22), (23) and (24). The calculation of fields far from the scatterer leads to some simplifications in these expressions. From figure 2 we see that the distance R , which is the distance from a point on the wire scatterer to the measurement point (receiver), is just

$$R^2 = r_r^2 + r_n^2 - 2r_r r_n \cos \xi_n, \quad \dots(35)$$

where r_n and r_r are the distances from the origin to the point n of the scatterer and to the receiver respectively while ξ_n is the angle subtended by these two points at the origin. In radar cross-section studies, for which CHAOS is designed, the distances R and r_r will be large so that we may expand R , keeping terms to $1/r_r$ only, to get from equations (23) and (28)

$$\underline{A}^s(\underline{r}_r) = \mu \frac{e^{-ikr_r}}{4\pi r_r} \sum_{i=1}^N I_i \int_{\text{wires}} \underline{T}_i(l) e^{ikr \cos \xi} dl, \quad \dots(36)$$

$$\phi^s(\underline{r}_r) = O\left(\frac{1}{r_r^2}\right). \quad \dots(37)$$

Thus, the components of the far electric field in a spherical coordinate system become

$$\begin{aligned} E_r &= O\left(\frac{1}{r_r^2}\right), & \} \\ E_\theta &\approx -i\omega A_\theta^s, & \} \\ E_\phi &\approx -i\omega A_\phi^s. & \} \end{aligned} \quad \dots(38)$$

The transverse component of the electric field at large distances is

$$\underline{E}^s \cdot \underline{u}_r = -i\omega\mu \frac{e^{-ikr_r}}{4\pi r_r} \sum_{i=1}^N I_i \int_{\text{wires}} \underline{u}_r \cdot \underline{T}_i(l) e^{ikr \cos \xi} dl, \quad \dots(39)$$

where \underline{u}_r is some unit vector transverse to \underline{r}_r , the direction of the receiver.

The program could be modified to give near fields as well as far but this has not been done. Should it ever be attempted in future, the fields close to the structure will exhibit singularities and may be unreliable since the charge distribution on the wire structure goes through a discontinuous change at the start and end of each triangle function. It would be necessary for very careful thought to be given to the problem of avoiding wrong results due to these discontinuities. It may only be possible to obtain fields on a grid of carefully chosen points close to the structure with interpolation being used for points not on the grid.

3.6 Radar cross-sections

The radar cross-section $g(\theta, \phi)$ is defined as the area for which the incident wave contains sufficient power to produce, by omnidirectional radiation, the same back scattered power density. So we have

$$g(\theta, \phi) = \frac{4\pi r^2}{\eta} \frac{|\underline{E}^s \cdot \underline{u}_r|^2}{P_{in}}, \quad \dots(40)$$

where the power of the incident wave P_{in} is

$$P_{in} = \frac{|\underline{E}_o|^2}{\eta}, \quad \dots(41)$$

$$= \frac{1}{\eta} \text{ for a unit plane wave,}$$

where $\eta = \sqrt{\frac{\mu}{\epsilon}}. \quad \dots(42)$

CHAOS will accept any polarisation, linear, elliptic or circular, for the incident plane wave and will calculate the radar cross-section for a receiver having any linear, elliptic or circular polarisation. The receiver need not be in the same place as the transmitter so that CHAOS will calculate bistatic as well as monostatic radar cross-sections.

3.7 Numerical evaluation of impedance matrix elements

The numerical evaluation of the impedance matrix elements given by equation (32) needs some explanation since the integrand contains a singularity and involves a double integration. Let us write Z_{ji} as

$$Z_{ji} = Z_{ji}^M + Z_{ji}^E + Z_{ji}^C, \quad \dots(43)$$

$$\text{where } Z_{ji}^M = i\omega\mu \int_{\text{wires}} dl \int_{\text{wires}} dl' \underline{T}_j(l) \cdot \underline{T}_i(l') \frac{e^{-ikR}}{4\pi R}, \quad \dots(44)$$

$$Z_{ji}^E = \frac{1}{i\omega\epsilon} \int_{\text{wires}} dl \int_{\text{wires}} dl' \frac{d}{dl} \underline{T}_j(l) \frac{d}{dl'} \underline{T}_i(l') \frac{e^{-ikR}}{4\pi R}, \dots(45)$$

$$Z_{ji}^C = \int_{\text{wires}} dl Z_{\omega i-j} \underline{T}_i(l). \quad \dots(46)$$

The three terms are due to the magnetic vector potential, the electric scalar potential and finite conductivity respectively which accounts for the superfixes of M, E and C. As each triangle function \underline{T}_i is non-zero only over four segments (see figure 1(a)), the integrations reduce to integrals over at most eight different segments. These are replaced by sums over these segments by representing the basis function and its derivative by a sum of four step functions, as illustrated in figure 3. The weight function and its derivative are replaced by a sum of four impulses, as shown in figure 4. This enables the double integrals in equations (44) and (45) to be replaced by a sum of sixteen terms as follows:-

$$Z_{ji}^M = i\omega\mu \sum_{m=1}^4 \sum_{n=1}^4 t_{jm} t_{in} D_{jm}^{in} \psi_{jm}^{in}, \quad \dots(47)$$

$$Z_{ji}^E = \frac{1}{i\omega\epsilon} \sum_{m=1}^4 \sum_{n=1}^4 t'_{jm} t'_{in} \psi_{jm}^{in}, \quad \dots(48)$$

where D_{jm}^{in} is the scalar product between the vectors in the directions $\underline{r}_{j,m+1} - \underline{r}_{j,m}$ and $\underline{r}_{i,n+1} - \underline{r}_{i,n}$ and where \underline{r}_{jm} is the vector from the origin to the start of segment m under triangle function j. This notation is illustrated in figure 5. Finally, the ψ function is defined as

$$\psi_{jm}^{in} = \frac{1}{4\pi(\ell_{2i-1+n} - \ell_{2i-2+n})} \int_{\ell_{2i-2+n}}^{\ell_{2i-1+n}} dl' \frac{e^{-ikR}}{R}, \quad \dots(49)$$

in which R is the distance between the field point adjacent to the midpoint of segment m under triangle function j and the source point on the n^{th} segment under triangle function i. The index m causes the

summation to extend over the four segments forming the base of triangle function j while the index n causes the summation to extend over the four segments forming the base of triangle function i . The formulae used to evaluate the integral in equation (49) have been derived by Harrington [8] and are tabulated in appendix A.

The alert reader will have noticed the use of the rather imprecise term "adjacent" in the previous paragraph. The integral in equation (49) contains a singularity when the field point coincides with a point on the line source. In order to remove this singularity, it has generally been decided to consider the line sources as situated on the axes of the wires while the field points are situated on the surfaces. The position of the field point on the wire surface is illustrated in figure 6 and is determined as follows: a line is drawn from the source point to the axis of the wire on whose surface the field point is to be situated. At right-angles to both this line and this axis, another line is drawn. This line cuts the wire surface in two points. One of these points is taken as the field point; while there is still ambiguity in which point is the field point, there is no ambiguity in the distance R . It is the same from both points. In the degenerate case of a field point on the same segment as the source, any point on the circumference will do and each point gives the same distance R .

For two reasons the impedance matrix calculated in the manner described here will no longer be exactly symmetric. The first is that the mathematical representation of the weighting function (shown in figure 4) is different from that used for the basis function (shown in figure 3). The second is the method of avoiding the singularity in equation (49). Harrington [2] has found that little difference is made to the radar cross-sections by averaging the off-diagonal elements of the impedance matrix. This has also been confirmed by our own calculations and this averaging is usually performed by CHAOS although the unsymmetric matrix can be used if desired by specifying the appropriate option. The advantages of symmetry are substantially reduced computer storage needs and the exact satisfaction of the principle of reciprocity.

3.8 Numerical evaluation of the voltage vector

The numerical evaluation of the voltage vector given by equation (31) is straightforward. In the CHAOS program the source is assumed to be a plane wave of the form

$$\underline{E}^i(\underline{r}) = \underline{E}_0 e^{-ik \cdot \underline{r}} \quad \dots(50)$$

The form of \underline{E}_0 determines the polarisation of the wave as described in appendix B. The weight function is represented by a set of impulse functions (as in figure 4) and so we get

$$V_j = \sum_{m=1}^k T_{jm} \Delta_{jm} \cdot \underline{E}_0 e^{-ik \cdot (\underline{r}_{j,m+1} + \underline{r}_{j,m})/2}, \quad \dots(51)$$

where Δ_{jm} is the vector representing the length and direction of the m^{th} segment of triangle function j .

4. JUNCTIONS OF WIRES

There are two conditions that must be satisfied at a junction. The first is Kirchoff's law which states that the sum of the currents entering a junction equals the sum of the currents leaving the junction. The second states that the scalar potential is continuous across the wire surfaces at the junction. Kirchoff's law is relatively easy to satisfy but the condition on scalar potential has not been satisfied in any computer program known to the author. This is because the unknown variables in method of moments solutions are the currents and their derivatives, the charges. Thus, we really need a condition on the charge not the scalar potential. It is possible to write down an analytical expression for the charge but it is not very suitable for a computer program. So various authors have put forward a variety of approximations.

Two in particular have been picked out and programmed into CHAOS but neither is entirely satisfactory so an approximation based on a combination of these two methods has also been programmed. Three other

ideas have also been tried out but are only of limited use. In none of these methods is it necessary to place further restrictions on the length of segment or radius of the wire abutting the junction than those which must be satisfied at any point of a wire, as described in appendix A.

4.1 Chao and Strait's method

The first approximation is used by both Chao and Strait [1] and Richmond [4]. Suppose N wires meet at some junction, then Kirchoff's law is satisfied exactly by overlapping wire i by two segments on to wire $i - 1$, except that wire 1 is not overlapped on to wire N . This is shown in figure 7(a) for three wires. This allows extra triangle functions on wires 2 and 3 which straddle the junction (these are labelled I_s and I_T in figure 7(a)). The total current $I(\ell)$ on a segment adjacent to a junction is the sum of the current on that segment and the extra overlap segment if it exists. The line density of charge is obtained from equation (19) which is

$$\sigma(\ell) = \frac{i}{\omega} \frac{dI(\ell)}{d\ell}.$$

As the wire connection data are read in, the program records in an array the wire numbers of all wires that enter each junction in the order in which they are encountered in the input data. This is slightly modified for problems with rotational symmetry (see section 7).

An aspect of this overlapping wire method that does not appeal to a mathematician is the asymmetry and arbitrariness introduced by having to choose one wire at each junction to have no overlap and by the choice of which order the remaining wires overlap each other. Two different people setting up the same problem will not necessarily number the wires and junctions in the same way so that a different set of overlaps will result and a different set of triangle functions will be set up. But the sum of the appropriate two triangle functions on a segment adjacent to a junction will still give the same total current - at least to within the accuracy of the calculation. This objection has a practical effect when dealing with a structure having left-right symmetry or N -fold rotational symmetry which is discussed further in section 7.

The only satisfactory way of removing this ambiguity is to do away with overlaps completely. However, this means an extra constraint (representing Kirchoff's law) must be introduced and this leads to an extra row in the impedance matrix whose elements may be of very different magnitudes since they do not represent impedances. Also for a triangle function basis, one must introduce right-angled triangle functions at the ends of each wire which complicates the programming. Thus, in CHAOS we generally use overlapping triangle functions and live with the arbitrariness. These overlaps are worked out automatically by the geometry package in the CHAOS program and the program user need not worry over this.

4.2 Sayre's method

The second method has been suggested by both Curtis [9] and Sayre [10] while an improved scheme has been put forward by King [11]. These methods all involve charge redistribution. One starts from equation (19) and at a junction of N wires integrates this over a small volume surrounding the junction. This volume is defined by the ends of the N segments abutting the junction. Sayre makes the assumption that the line density of charge is constant over these N segments and arrives at the expression

$$\bar{\sigma} = \frac{i}{\omega} \frac{\sum_{i=1}^N I(\ell_{\omega_i})}{\sum_{i=1}^N \Delta_{\omega_i}}, \quad \dots(52)$$

where ℓ_{ω_i} is the position of the other end of the segment abutting the junction on wire ω_i and Δ_{ω_i} is the length of this segment. Now because of the overlaps used to satisfy Kirchoff's law, there would appear to be $2N - 1$ segments abutting a junction of N wires. For the purpose of representing this average charge, the $N - 1$ segments due to overlaps are ignored and no charge is spread over them. The charge is then spread uniformly over the N segments adjacent to the junction which were on the original wires.

Curtis's scheme made the assumption that the surface density of charge was constant, while King, working with a tapered wire, produces two formulae, one for short wires the other for long ones. In the limit of wires of equal radius King's formula reduces to Sayre's showing that there is some justification for assuming that the line density of charge is constant. However, King's scheme has not been programmed because it is known that Sayre's treatment does not always give acceptable results for junctions of wires of equal radius.

4.3 50/50 method

Since neither Chao and Strait's nor Sayre's methods always give acceptable results, a new scheme was tried. It has been noticed that when Chao and Strait's method disagrees with experiment, Sayre's method usually gives acceptable results. The converse also appears to hold. Thus, it was decided to calculate the charge by both methods and combine them with equal weight to give the formula

$$\frac{1}{2} \sigma(\ell) + \frac{1}{2} \bar{\sigma}. \quad \dots(53)$$

Thus, in calculating the charge, one is taking account of both the individuality of the wire and of the aggregate of wires meeting at the junction. No attempts have been made to optimize the expression (53) by choosing different weightings (eg, 30/70, 80/20, etc).

4.4 Other methods

It has been noticed that the Chao and Strait method is generally better for wire meshes representing solid surfaces while the 50/50 method is generally better for junctions of actual wires. For these reasons an option is provided in CHAOS which allows certain junctions to use Chao and Strait's methods and others to use the 50/50 method.

In another scheme the currents on all wires entering a junction are forced to be zero. This means that the overlapping segments are not

required. Sayre's method for charge redistribution is used. Surprisingly, this scheme gives good results for some geometries; however, its use is not recommended.

Finally, a more promising method without overlaps is programmed. In this scheme, each triangle function abutting a junction of two or more wires was replaced by a step function on the two segments adjacent to the junction, as shown in figure 7(b), while Sayre's charge redistribution scheme is used. The saving in matrix size gained by the simpler junction treatment was offset by the need for more segments along each wire. The method required 6 and preferably 8 segments between any two junctions whereas the 50/50 method only needed 2 on the same problem. Also Kirchoff's law is not satisfied exactly so, for these reasons, the method has not been pursued but it has been left in the CHAOS program.

4.5 Effects on impedance matrix elements

As the Chao and Strait junction method does not involve charge re-distribution, it does not affect the way the impedance matrix elements are calculated, but all the other methods do. Of the three terms that the impedance matrix elements have been split into, it is only that due to the electric scalar potential that is affected. The factor $(d/d\ell')T_i(\ell')$ in equation (45) and t_{in}^i in equation (48) need to be replaced. In order to see the form these take let us suppose that at some junction of N wires, triangle functions J_1 to J_{N_1} are directed out of the junction (ie, leave the junction), K_1 to K_{N-1} straddle the junction (ie, are overlaps) and L_1 to L_{N_2} are directed into the junction (ie, enter the junction). As N wires meet at the junction, $N_1 + N_2 = N$. Now the current leaving the volume surrounding the junction (as defined in section 4.2) is given by

$$\begin{aligned}
 I &= \sum_{i=1}^N I(\omega_i), \\
 &= \sum_{j=J_1}^{J_{N_1}} T_j(\ell_{2j}) I_j + \sum_{j=K_1}^{K_{N-1}} (T_j(\ell_{2j+2}) - T_j(\ell_{2j})) I_j - \sum_{j=L_1}^{L_{N_2}} T_j(\ell_{2j+2}) I_j. \\
 &\qquad \qquad \qquad \dots (54)
 \end{aligned}$$

From the form of equation (54) it is clear that the modification will affect $2N - 1$ columns of the impedance matrix since for Sayre's method equation (45) becomes

$$Z_{ji}^E I_i = \frac{1}{i\omega\epsilon} \int_{\text{wires}} dl \int_{\text{wires}} dl' \frac{e^{-ikR}}{4\pi R} \frac{d}{dl} T_j(l) \\ \times \left\{ a(l') \frac{d}{dl'} T_i(l') I_i + b(l') \frac{I}{\sum_{p=1}^N \Delta_{\omega p}} \right\}, \quad \dots(55)$$

where I is given by equation (54). The $a(l')$ and $b(l')$ are defined by:-

$$a(l') = \begin{cases} 1 & \text{normally,} \\ 0 & \text{if } l' \text{ is on a segment adjacent to a junction,} \end{cases} \\ b(l') = \begin{cases} 0 & \text{normally,} \\ 1 & \text{if } l' \text{ is on a wire segment (not an overlap segment)} \\ & \text{adjacent to a junction.} \end{cases}$$

This formula, equation (55), is not quite general since a triangle function can leave, straddle and enter three junctions (see figure 8) although only two junctions will contribute to the average charge since we have decided not to spread any charge on an overlap segment (section 3.2). So a further term in the curly brackets is required similar to the $b(l')$ term but referring to this second junction.

The equation corresponding to equation (48) is

$$Z_{ji}^E I_i = \frac{1}{i\omega\epsilon} \sum_{m=1}^4 \sum_{n=1}^4 t'_{jm} \{ a_i(n) t'_{in} I_i + b_i(n) Q \} \psi_{jm}^{in}, \quad \dots(56)$$

$$\text{where } Q = \frac{(\ell_{2i-1+n} - \ell_{2i-2+n})}{2 \sum_{p=1}^N \Delta_{\omega p}} \left[\sum_{j=J_1}^{J_{N_1}} t'_{j1} I_j + \sum_{j=L_1}^{L_{N_2}} t'_{j4} I_j \right]. \quad \dots(57)$$

The terms involving the K type triangle functions (ie, those that straddle the junction) are identically zero because the program, as it is at present set up, makes all segments between any two junctions equal in length. Should this be changed in future, then an extra term will need to be added into equation (57). From figure 9 we see that:-

$$\begin{aligned}
 a_i(n) &= 1 \quad \text{normally,} \\
 &= 0 \quad \text{if triangle function } i \text{ leaves a junction } J \text{ and } n = 1 \\
 &\quad \text{(cases (i) and (ii)),} \\
 &= 0 \quad \text{if triangle function } i \text{ straddles a junction } K \text{ and } \\
 &\quad n = 2 \text{ or } 3 \text{ (cases (iii) and (iv)),} \\
 &= 0 \quad \text{if triangle function } i \text{ enters a junction } L \text{ and } n = 4 \\
 &\quad \text{(cases (v) and (vi)),}
 \end{aligned}$$

and:-

$$\begin{aligned}
 b_i(n) &= 0 \quad \text{normally,} \\
 &= 1 \quad \text{if triangle function } i \text{ leaves a junction } J \text{ and if} \\
 &\quad \text{wire on which } i \text{ is situated has no overlap at } J \\
 &\quad \text{and if } n = 1 \text{ (case (i)),} \\
 &= 1 \quad \text{if triangle function } i \text{ straddles a junction } K \\
 &\quad \text{and either } n = 2 \text{ if wire enters junction (case (iii))} \\
 &\quad \text{or } n = 3 \text{ if wire leaves junction (case (iv)),} \\
 &= 1 \quad \text{if triangle function } i \text{ enters a junction } L \text{ and if} \\
 &\quad \text{wire on which } i \text{ is situated has no overlap at } L \\
 &\quad \text{and if } n = 4 \text{ (case (vi)).}
\end{aligned}$$

In retrospect, the situations for which $b_i(n)$ are non-zero could be more logically chosen. One might argue that in case (ii) $b_i(1) = 1$, while in case (iv) $b_i(3) = 0$, and similarly in case (v) $b_i(4) = 1$, with case (iii) $b_i(2) = 0$. Alternatively, one might argue that in cases (ii) and (iv) $b_i(1) = p$ and $b_i(3) = 1 - p$ respectively with a similar split for cases (v) and (iii). One would perhaps like to choose this weight p as the ratio of current magnitude due to one triangle function to the sum of the magnitudes of the two triangle functions which are based on the segment adjacent to the junction. However, this produces a non-linear problem and is to be avoided. For better or for worse, we have chosen this weight p to be zero and no study has been made of other alternatives; perhaps one day this should be done.

As with equation (55), expression (56) is not quite general since two of the situations listed above could occur simultaneously. This could arise since we know from figure 8 that a triangle function can

leave a junction J, straddle a junction K and enter a junction L. As depicted there would be contributions to triangle functions i from both junctions J and K but not L. The converse could also happen in which contributions from junctions L and K occurred but not J. The third possibility arises when a triangle function leaves a junction J, does not straddle any junction but enters another junction L. Thus, another term of the type $b_i(n)Q$ referring to this second junction needs to be included in the curly brackets of equation (56).

However, the 50/50 method produces a further complication; expressions (56) and (57) remain the same but the coefficients $a_i(n)$ and $b_i(n)$ are modified. Where the parameter $a_i(n) = 0$ in the Sayre formulation it is set to 0.5 in the 50/50 method. Similarly, where the parameter $b_i(n) = 1$ in the Sayre formulation it is set to 0.5 in the 50/50 method.

Finally, it is clear from equation (56) that the resulting matrix Z_{ji}^E will be unsymmetric since the original symmetric matrix has been replaced by a matrix whose columns are linear combinations of the original columns without any corresponding replacement of rows. The Harwell matrix factorization package MA23 is used for this situation. More recently tests have suggested that the result of averaging the off diagonal terms to force the matrix Z_{ji}^E to be symmetric is in no worse agreement with experiment and in some ways is in rather better agreement (in the sense that reciprocity is satisfied). Thus, the option exists to force the matrix to be symmetric and, in view of the saving in computer storage that follows from this, it is now the recommended option.

5. WIRE MESH MODELLING OF SOLID SURFACES

On the face of it a computer program based on the thin wire approximation is inappropriate for calculations involving surfaces. However, it is believed that at present no reliable general purpose surface patch computer code has been written which can cope with finite conductivity or which results in a symmetric impedance matrix. The reason for this is essentially that the calculation of the elements of the

impedance matrix would be very expensive and perhaps difficult as the expression analogous to equation (32) involves a four-fold rather than a two-fold integral. Intuitively, one feels that a smaller, perhaps much smaller, matrix would result so that for problems involving many aspect angles and polarisation combinations, a surface patch approach might be viable.

So how does one use CHAOS to model a surface of a conductor which is not necessarily a perfect conductor? The trick is to recall that a wire mesh in the same shape as a solid surface will give very similar radar cross-sections provided the mesh size is small compared with the wavelength. Thus, one replaces the solid surface by a wire mesh whose holes are roughly 0.02 to 0.03 square wavelengths in area. This size has been determined by experience. The main worry with this approach is that one is forcing the currents to flow along the wires of the mesh rather than as they would in real life. For this reason a triangular mesh rather than a rectangular one is preferred. Also one would tend to use a finer mesh on surfaces of high curvature than on flat surfaces, and at edges of surfaces where larger currents might be expected to flow. Should any part of the surface suggest a preferred direction for the current to flow, then the mesh sides should be aligned in this direction.

Next, there is the question of what radius to give the wires in the mesh. Experience has again shown that this should be chosen so that the surface area of the wire mesh is no less than the area of the solid surface. In this way the position of the lobes of the radar cross-section pattern will be correctly predicted. However, only the amplitude of the major lobes will be reliably calculated. If the radius has not been correctly chosen, one may expect errors in amplitude of a few decibels for lobes 10 db below the maximum while for smaller lobes, say 20 to 30 db below the maximum, errors of 5 to 10 db have been seen. In many applications this sort of accuracy is quite acceptable. So no exact prescription can be given for the radius of the wires in the mesh and up to five times that suggested above may be necessary to get good agreement with experiment on the minor lobe amplitudes. This sort of variation in wire mesh radius has very little effect on the amplitudes of the major lobes, perhaps of the order of a decibel.

The wires should be given the same conductivity as the solid surface. In the case where the surface is composed of strips of material having different conductivities along and across the strips, then the mesh should be rectangular in shape aligned along and across the strips, the wires in one direction having one conductivity, the ones in the other the other conductivity.

Finally, we have found that the Chao and Strait junction treatment for wires in meshes representing solid surfaces tends to give much better predictions for minor lobes than does Sayre's treatment.

6. TREATMENT OF MATERIALS WHICH ARE NOT PERFECTLY CONDUCTING

6.1 Types of current

At this point one must consider the various types of complex current density. Inside a conductor, the current is almost entirely due to the motion of free electrons and is called the conduction current and is given by

$$\underline{J} = \sigma \underline{E}, \quad \dots(58)$$

where σ is the conductivity.

In free space we have no motion of charges at all and we have only a "free space displacement current" given by

$$i\omega \epsilon_0 \underline{E}, \quad \dots(59)$$

where ϵ_0 is the dielectric constant of free space ($\approx (1/36\pi) \times 10^{-9}$ F/m).

In matter, in addition to the conduction current and the free space displacement current, there is a current due to the motion of the bound charges. This is called the polarisation current and is given by

$$i\omega(\epsilon - \epsilon_0) \underline{E}. \quad \dots(60)$$

For completeness one should note that the current $i\omega\mathbf{E}$ is called the displacement current.

Both the conduction and polarisation currents give rise to scattered electric fields due to the motion of the charges. So for a non-magnetic material we would like to calculate both these currents. Let us write

$$\underline{\mathbf{J}}^s = \underline{\mathbf{J}} + i\omega(\epsilon - \epsilon_0)\underline{\mathbf{E}}, \quad \dots(61)$$

then $\underline{\mathbf{J}}^s$ gives rise to the total scattered field for a non-magnetic material.

6.2 Impedance of wire

By substituting for $\underline{\mathbf{J}}$ from equation (58) into the third of equations (6) and also using the first we have

$$\nabla \wedge \nabla \wedge \underline{\mathbf{E}} - T^2 \underline{\mathbf{E}} = 0, \quad \dots(62)$$

where $T^2 = -i\omega\mu(\sigma + i\omega\epsilon)$. Clearly, we also have

$$\nabla \wedge \nabla \wedge \underline{\mathbf{J}} - T^2 \underline{\mathbf{J}} = 0 \quad \dots(63)$$

and so $\nabla \wedge \nabla \wedge \underline{\mathbf{J}}^s - T^2 \underline{\mathbf{J}}^s = 0. \quad \dots(64)$

Now let us specialize to a cylindrical wire of infinite length lying along the Z axis. Let us assume the current only flows in the Z direction and is a function of ρ , the radial distance only. Let us use cylindrical polar coordinates (ρ, ϕ, Z) based on the Z axis. Then

$$\underline{\mathbf{J}}^s = (0, 0, J(\rho)) \quad \dots(65)$$

and equation (64) reduces to

$$\frac{1}{\rho} \frac{d}{d\rho} \left(\rho \frac{dJ}{d\rho} \right) + T^2 J = 0. \quad \dots(66)$$

This is Bessel's equation. We require that solution which is finite at the centre and which gives the current density i_0 , say, at the surface of the wire. So

$$J(\rho) = i_0 \frac{J_0(T\rho)}{J_0(Ta)}, \quad \dots(67)$$

where a is the radius of the wire and J_0 is the cylindrical Bessel function of order zero which is regular at the origin.

The total current, I , flowing in the wire is given by

$$\begin{aligned} I &= \int_0^{2\pi} d\phi \int_0^a \rho d\rho J(\rho), \\ &= i_0 \frac{2\pi a}{T} \cdot \frac{J_1(Ta)}{J_0(Ta)}, \end{aligned} \quad \dots(68)$$

where J_1 is the cylindrical Bessel function of order unity which is regular at the origin. The electric field at the wire surface is given by

$$E_\omega = \frac{i_0}{(\sigma + i\omega(\epsilon - \epsilon_0))} = Z_\omega I, \quad \dots(69)$$

where the wire impedance per unit length Z_ω is given by

$$Z_\omega = \frac{T}{2\pi a(\sigma + i\omega(\epsilon - \epsilon_0))} \frac{J_0(Ta)}{J_1(Ta)}. \quad \dots(70)$$

It has been found that this formula is inadequate for some materials, in particular those which are not solid but consist of strands of fibre woven together. For these materials the amended formula

$$Z_\omega = \frac{T}{2\pi a(\sigma + i\omega(\epsilon - \epsilon_0))} \cdot \frac{J_0(Ta)}{J_1(Ta)} \left(1 + \frac{\omega}{2\pi\nu}\right) \quad \dots(71)$$

is used where ν is the "frequency fit" parameter in cycles per second and is chosen to give optimum agreement with experimental impedance per unit length data.

The use of this formula has been found to give good radar cross-sections for "wires" ranging from copper ($\sigma = 5.8 \times 10^7$ mho/m) to salt water ($\sigma = 20.37$ mho/m, $\epsilon = 50\epsilon_0$) and polystyrene ($\epsilon = 2.54\epsilon_0$, loss tangent = 4.05×10^{-4}).

No computer routines have been found that will accurately calculate the Bessel functions J_0 and J_1 for an arbitrary complex argument, ζ ; however the ratio J_1/J_0 can be found satisfactorily for all arguments from the continued fraction (12)

$$\frac{J_1(\zeta)}{J_0(\zeta)} = \frac{\zeta}{2 - \frac{\zeta^2}{2(q+1) - \frac{\zeta^2}{2(q+2) - \frac{\zeta^2}{2(q+3) - \zeta^2}}}} \quad \dots(72)$$

For large $|\zeta|$ we have

$$\begin{aligned} \frac{J_1(\zeta)}{J_0(\zeta)} &= \frac{\cos(\zeta - \frac{3}{2}\pi)}{\cos(\zeta - \frac{1}{2}\pi)} + O(\zeta^{-1}), \\ &\approx i \text{ for large } \text{Im}(\zeta) > 0, \\ &\approx -i \text{ for large } \text{Im}(\zeta) < 0. \end{aligned} \quad \dots(73)$$

For small $|\zeta|$ we have

$$\frac{J_1(\zeta)}{J_0(\zeta)} \approx \frac{1}{2} \zeta. \quad \dots(74)$$

Some other quantities are perhaps worth recording. The skin depth, δ , is given by

$$\delta = \sqrt{\frac{2}{\omega\mu\sigma}}. \quad \dots(75)$$

The loss tangent is the ratio of imaginary to real components of the dielectric constant and the loss angle η is given by

$$\tan \eta = \frac{\text{Im}(\epsilon)}{\text{Re}(\epsilon)}. \quad \dots(76)$$

The resistance R_ω and inductance L_ω per unit length are related to Z_ω by

$$R_\omega + i\omega L_\omega = Z_\omega. \quad \dots(77)$$

The dc resistance and inductance per unit length are given by

$$R_{DC} = \frac{1}{\pi\sigma a^2} \quad \dots(78)$$

and $L_{DC} = \frac{\mu}{8\pi}$ (= 50 nH/m). \dots(79)

At high frequency and provided $\sigma \gg \omega\epsilon$, we have approximately

$$R \approx \omega L \approx \frac{1}{\pi a} \sqrt{\frac{\omega\mu}{8\sigma}} \left(1 + \frac{\omega}{2\pi\nu}\right). \quad \dots(80)$$

6.3 Form of matrix of contributions due to finite conductivity

The matrix of contributions due to finite conductivity is given by substituting equation (71) into equation (46). Because the current basis functions are a set of overlapping triangles, this matrix is sparse with most contributions on or immediately adjacent to the main diagonal. In the special case of a dipole the matrix is tridiagonal, but for problems involving three or more wires joined at a vertex this ceases to be so and contributions outside the diagonal band occur. Since the programming required to calculate correctly these contributions is somewhat involved, it would have been easier to treat finite conductivity as a series of lumped loads situated at the centres of each triangle function which leads to a nearly diagonal matrix. Although this has been done in other computer programs, this slightly less realistic approach has not been adopted in CHAOS.

6.4 Lumped loads

Some problems involve the attachment of loads to the scattering body and so an option is provided to allow these to be included. These might take the form

$$Z_L = R + i\omega L - \frac{1}{i\omega C}, \quad \dots(81)$$

where R, L and C are respectively resistance, inductance and capacitance. In CHAOS such loads may be attached either at the beginning of a wire or at the end of an even numbered segment. This means that the load is attached in series between the two segments. A load attached at a free end of a wire will have no effect since the current is assumed to be zero at free ends.

The effect on the impedance matrix is to alter the diagonal term corresponding to the triangle function at whose centre the load is attached. At wire junctions where three or more wires meet, the load may be attached at the centre of two triangle functions thus affecting two diagonal terms and an off diagonal term. For instance, in figure 7(a), if a load were attached at the end of wire 2 which enters the junction, then the S and T diagonal elements of the impedance matrix will be affected as well as the ST off diagonal element. This is because both triangle functions I_S and I_T have a common centre at the end of wire 2.

Another unwelcome feature of lumped loads is that the impedance matrix can become badly scaled as a result of adding in these loads. Experience shows that the impedance matrix should be properly scaled before factorization but even this may not be sufficient for computers with a short word length (eg, 32 bits) and errors of up to 0.5 db have been seen in the peak values of some lobes. Thus, jobs involving loaded structures should ideally be run on computers with a longer word length (eg, 64 bits).

7. SYMMETRIES IN GEOMETRICAL STRUCTURE

In some problems the geometrical structure possesses special symmetries which can be utilised to reduce substantially computing time and storage. We consider first the case of a body with rotational symmetry, eg, a cylinder; then a body with left-right symmetry, eg, an aircraft; and finally a body with two planes of mirror symmetry, eg, an aircraft sitting on a perfectly conducting ground plane.

7.1 Rotational symmetry

Let us consider a body with n-fold rotational symmetry about some axis. In the CHAOS program this axis is required to be the Z axis but the following analysis does not depend on this. Let us divide the structure up into n sections, together with a section describing those triangle functions lying wholly on the axis of rotation. Then the impedance matrix may be written in block matrix form as:-

$$Z = \begin{bmatrix} Z_B & Z_A^T & Z_A^T & Z_A^T \\ Z_A & Z_{11} & Z_{12} & Z_{1n} \\ Z_A & Z_{21} & Z_{22} & Z_{2n} \\ & & \cdot & \\ Z_A & Z_{n1} & Z_{n2} & Z_{nn} \end{bmatrix} \quad \dots(82)$$

where the square matrix Z_B represents the interactions between triangle functions lying wholly along the axis of rotation, the square matrix Z_{ij} represents the interactions between section i and section j of the structure, and the rectangular matrix Z_A represents interactions between the axis and any one of the n sections. The matrix Z is assumed to be symmetric so that $Z_{ij} = Z_{ji}^T$ where T denotes transpose. This means that a junction treatment which gives rise to a symmetric impedance matrix must be used. We could have done the analysis with an unsymmetric matrix Z but this requires roughly twice as much storage and does not guarantee that the principle of reciprocity is satisfied. We can immediately write down some relations between the blocks Z_{ij} due to the rotational symmetry of the geometry. These are

$$Z_{ij} = \begin{cases} Z_{n+j-i+1} & \text{for } i > j, \\ Z_{j-i+1} & \text{for } i \leq j, \end{cases} \quad \dots(83)$$

where Z_k is the interaction between a section l and a section $l + k - 1$. Due to the symmetry of the whole matrix Z we have $Z_{ij} = Z_{ji}^T$ and so obtain the further relation

$$Z_{n-k+1}^T = Z_{k+1} \quad k = 1, 2, \dots, n - 1. \quad \dots(84)$$

So in the case where n is even and equal to $2q$, say, we have

$$Z_{q+1}^T = Z_{q+1}, \quad \dots(85)$$

ie, Z_{q+1} is symmetric. Thus, for storage purposes, we only require space for the matrices $Z_B, Z_A, Z_1, Z_2, \dots, Z_{r+1}$ where r is the integer part of $n/2$. Of these matrices Z_B, Z_1 and, for $n=2q$, Z_{q+1} are symmetric.

Now let us write the current and voltage vectors in a similar block form as:-

$$\underline{I} = \begin{bmatrix} \underline{I}_B \\ \underline{I}_1 \\ \underline{I}_2 \\ \cdot \\ \cdot \\ \cdot \\ \cdot \\ \underline{I}_n \end{bmatrix} \quad \text{and} \quad \underline{V} = \begin{bmatrix} \underline{V}_B \\ \underline{V}_1 \\ \underline{V}_2 \\ \cdot \\ \cdot \\ \cdot \\ \cdot \\ \underline{V}_n \end{bmatrix} \quad \dots(86)$$

Also let us define the quantity

$$S_{jk} = e^{2\pi i(j-1)(k-1)/n} \quad j, k = 1, 2, \dots, n. \quad \dots(87)$$

Then we see that

$$\begin{aligned}
 S_{j+l-1,k} &= S_{jk} S_{lk}, \\
 S_{j-l+1,k} &= S_{jk} S_{lk}^*, \text{ where } * = \text{complex conjugate}, \\
 S_{j+n,k} &= S_{j,k}, \\
 \sum_{k=1}^n S_{jk} S_{lk}^* &= \begin{cases} n & \text{if } j = l, \\ 0 & \text{otherwise.} \end{cases}
 \end{aligned}
 \tag{88}$$

We may now expand the matrix equation $Z\underline{I} = \underline{V}$ to obtain

$$\begin{aligned}
 Z_{B \rightarrow B} \underline{I} + Z_A^T \left(\sum_{j=1}^n \underline{I}_j \right) &= \underline{V}_B, \\
 Z_{A \rightarrow B} \underline{I} + \sum_{j=1}^n Z_{ij} \underline{I}_j &= \underline{V}_i \quad i = 1, 2, \dots, n.
 \end{aligned}
 \tag{89}$$

We now multiply the i^{th} equation of this latter set by S_{ki} and sum over i to obtain

$$\left(\sum_{i=1}^n S_{ki} \right) Z_{A \rightarrow B} \underline{I} + \sum_{i=1}^n \sum_{j=1}^n S_{ki} Z_{ij} \underline{I}_j = \sum_{i=1}^n S_{ki} \underline{V}_i \quad k = 1, 2, \dots, n.
 \tag{90}$$

$$\text{Write } \underline{J}_k = \sum_{j=1}^n S_{jk} \underline{I}_j \tag{91}$$

$$\text{and } \underline{W}_k = \sum_{j=1}^n S_{jk} \underline{V}_j, \tag{92}$$

where \underline{J}_k and \underline{W}_k are discrete Fourier transforms of the currents \underline{I}_j and voltages \underline{V}_j . The inverse transformations give

$$\underline{I}_j = \frac{1}{n} \sum_{k=1}^n S_{jk}^* \underline{J}_k \tag{93}$$

$$\text{and } \underline{V}_j = \frac{1}{n} \sum_{k=1}^n S_{jk}^* \underline{W}_k. \tag{94}$$

Substituting for \underline{I}_j and \underline{V}_j we get

$$n\delta_{k1} Z_{A \rightarrow B}^{\underline{I}} + \frac{1}{n} \sum_{\ell=1}^n \sum_{i=1}^n S_{ki} Q_{\ell i}^{\underline{J}} = \underline{W}_k \quad k = 1, 2, \dots, n, \dots(95)$$

where $Q_{\ell i} = \sum_{j=1}^n S_{j\ell}^* Z_{ij}$ (96)

By substituting for Z_{ij} and doing some rearrangement of the summation we find

$$Q_{\ell i} = S_{i\ell}^* \sum_{p=1}^n S_{p\ell}^* Z_p \quad \dots(97)$$

So we want to solve the equations

$$n\delta_{j1} Z_{A \rightarrow B}^{\underline{I}} + \left(\sum_{p=1}^n S_{pk}^* Z_p \right)_{\underline{J}} = \underline{W}_k \quad k = 1, 2, \dots, n \quad \dots(98)$$

and $Z_{B \rightarrow B}^{\underline{I}} + Z_{A \rightarrow B}^{\underline{J}} = \underline{V}_B$ (99)

For $k = 2, 3 \dots, n$ we solve the block diagonal system of equations

$$U_{k \rightarrow k}^{\underline{J}} = \underline{W}_k, \quad \dots(100)$$

where $U_k = \sum_{p=1}^n S_{pk}^* Z_p$ (101)

while for $k = 1$ we solve the augmented equation

$$\begin{bmatrix} \frac{1}{n} Z_B & Z_A^T \\ Z_A & \sum_{p=1}^n Z_p \end{bmatrix} \begin{bmatrix} \underline{nI}_B \\ \underline{J}_1 \end{bmatrix} = \begin{bmatrix} \underline{V}_B \\ \underline{W}_1 \end{bmatrix} \quad \dots(102)$$

We now wish to examine the properties of the matrices U_k and in particular ask whether U_k is symmetric and whether any are related to each other. Now $U_k^T = \sum_{p=1}^n S_{pk}^* Z_p^T$ and after some rearrangement we obtain

$$U_k^T = \sum_{p=1}^n S_{pk} Z_p \quad \dots(103)$$

Hence, only U_1 and U_{q+1} if $m = 2q$ are symmetric; the rest are unsymmetric. Next let us consider

$$U_{n-r+2}^T = \sum_{p=1}^n S_{p,n-r+2} Z_p. \quad \dots(104)$$

After some manipulation we find

$$U_{n-r+2}^T = U_r. \quad \dots(105)$$

So for storage purposes we only require space for the matrices $(1/n) Z_B$, Z_A , U_1 , U_2 , ... U_{r+1} where r is the integer part of $n/2$. Of these matrices $(1/n) Z_B$, U_1 and, for $n = 2q$, U_{q+1} are symmetric. Thus, no more storage is required for this set of matrices than for the original set and the two sets can share the same storage area since the original set are never required again once the U_i are calculated.

All these transformed matrices are factorised either by MA29 if they are symmetric or by MA23 if they are not. A new routine, MA23T, has been written to solve for the system $A^T \underline{x} = \underline{y}$ where the factorization of the unsymmetric matrix A is known, since the Harwell package does not include this possibility.

The only other problem concerns the triangle functions which overlap from one section to the next. Such triangle functions must exist otherwise each section will be electrically isolated from the other. The geometry package in the CHAOS program has been modified to provide these overlaps automatically. To this end a convention has been adopted in which these overlaps are attached to the left-hand side of a section. This is illustrated in figure 10(a). A further modification to the CHAOS geometry package is required to ensure that wires attached to the axis of symmetry have their overlap connections arranged symmetrically. This is done by ensuring that each such wire has an overlap on to the axis, as illustrated in figure 10(b). This means that if a set of wires meet on the axis, then there must be another wire lying along the axis on to which the set of wires must overlap. If such an axis wire does not exist, then due to the method of attaching overlaps (described in section 4.1),

a symmetric system of overlaps cannot be set up. This problem could be got round by placing the unsymmetric set of triangle functions, due to this junction on the axis, into the matrix Z_B . However, this has not been programmed, as it would cause further problems in that the column of matrices Z_A in matrix (82) would have to be replaced by a column of unequal matrices. This would wreck the analysis that has been described here.

7.2 Left-right symmetry

This section is included although, at the time of writing, the option is not part of the CHAOS program. A plane must be chosen to be the mirror plane. As it is envisaged that aircraft will be one of the more important bodies for which this facility is useful, it is assumed that the mirror plane is the XZ plane. This does not affect the analysis given here but will affect the computer programming.

The matrix takes the form

$$Z = \begin{bmatrix} Z_B & Z_A^T & Z_A^T \\ Z_A & Z_1 & Z_2^T \\ Z_A & Z_2 & Z_1 \end{bmatrix}, \quad \dots(106)$$

where the square matrix Z_B now represents the interactions between triangle functions lying wholly in the mirror plane or which symmetrically straddle the plane. The square matrix Z_1 represents the interactions between triangle functions on one side of the mirror plane, while the square matrix Z_2 represents the interactions between triangle functions on one side of the plane with those on the other side. Lastly, the rectangular matrix Z_A represents the interaction between triangle functions in the plane (or straddling the plane) and those on one side of the plane. Once again the analysis is restricted to symmetric impedance matrices so that storage is saved and the principle of reciprocity is satisfied. The manner in which equation (106) is written implies that the numbering scheme on one side of the boundary is a reflection of that on the other. This implies too that the matrix Z_2 is itself symmetric, so that

$$\underline{Z}_2^T = \underline{Z}_2. \quad \dots(107)$$

The corresponding current and voltage vectors are written as

$$\underline{I} = \begin{bmatrix} \underline{I}_{-B} \\ \underline{I}_1 \\ \underline{I}_2 \end{bmatrix} \quad \text{and} \quad \underline{V} = \begin{bmatrix} \underline{V}_{-B} \\ \underline{V}_1 \\ \underline{V}_2 \end{bmatrix}. \quad \dots(108)$$

We define

$$\begin{aligned} \underline{J}_1 &= \underline{I}_1 + \underline{I}_2, & \underline{W}_1 &= \underline{V}_1 + \underline{V}_2, \\ \underline{J}_2 &= \underline{I}_1 - \underline{I}_2, & \underline{W}_2 &= \underline{V}_1 - \underline{V}_2, \\ \underline{U}_1 &= \underline{Z}_1 + \underline{Z}_2, & \underline{U}_2 &= \underline{Z}_1 - \underline{Z}_2, \end{aligned} \quad \dots(109)$$

then the equations we wish to solve, analogous to equations (100) and (102), are

$$\underline{U}_2 \underline{J}_2 = \underline{W}_2, \quad \dots(110)$$

$$\begin{bmatrix} \frac{1}{2} \underline{Z}_B & \underline{Z}_A^T \\ \underline{Z}_A & \underline{U}_1 \end{bmatrix} \begin{bmatrix} 2\underline{I}_{-B} \\ \underline{J}_1 \end{bmatrix} = \begin{bmatrix} \underline{V}_{-B} \\ \underline{W}_1 \end{bmatrix}. \quad \dots(111)$$

We then obtain

$$\begin{aligned} \underline{I}_1 &= \frac{1}{2} (\underline{J}_1 + \underline{J}_2), \\ \underline{I}_2 &= \frac{1}{2} (\underline{J}_1 - \underline{J}_2). \end{aligned} \quad \dots(112)$$

Now since \underline{Z}_1 and \underline{Z}_2 are symmetric, \underline{U}_1 and \underline{U}_2 are symmetric and advantage should be taken of this to save storage. As the matrix in equation (111) is symmetric, the Harwell routine MA29 may be used for all the factorizations.

Once again this section is provided although the programming has not yet been done. It is included because, for an aircraft sitting on a perfectly conducting ground plane, we have both the left-right symmetry of the aircraft and its reflection in the ground plane. This method would be invalid for a ground plane of finite conductivity. Following section 7.2, the left-right plane may be thought of as the XZ plane and the ground plane as the XY plane, but this does not affect the analysis given below.

The matrix takes the form

$$Z = \begin{bmatrix} Z_B & Z_A^T & Z_A^T & Z_A^T & Z_A^T \\ Z_A & Z_1 & Z_2^T & Z_3^T & Z_4^T \\ Z_A & Z_2 & Z_1 & Z_4^T & Z_3^T \\ Z_A & Z_3 & Z_4 & Z_1 & Z_2^T \\ Z_A & Z_2 & Z_3 & Z_2 & Z_1 \end{bmatrix} \dots(113)$$

It may be understood by reference to figure 11. Yet again the square matrix Z_B represents the interactions between triangle functions lying wholly in one or other mirror plane or which symmetrically straddle one or other plane. The square matrix Z_1 represents the interaction between triangle functions lying exclusively in one of the four sections. The square matrices Z_2 , Z_3 and Z_4 represent the interaction between triangle functions lying wholly in section 1 with those lying wholly in sections 2, 3 and 4 respectively. They also represent permutations of the above, eg, Z_2 also represents the interaction between sections 3 and 4, Z_3 between 2 and 4, and Z_4 between 2 and 3. Once again the numbering within each section must follow the numbering in the first section. In this way the four matrices Z_1 , Z_2 , Z_3 and Z_4 are all themselves symmetric provided that the original matrix Z is symmetric. Lastly, the rectangular matrix Z_A represents the interactions between triangle functions in the mirror planes (or straddling it) and one of the four sections.

In view of the above we have

$$\underline{Z}_i^T = Z_i, \quad i = 1, 2, 3, 4. \quad \dots(114)$$

The corresponding current and voltage vectors are written as

$$\underline{I} = \begin{bmatrix} \underline{I}_{-B} \\ \underline{I}_1 \\ \underline{I}_2 \\ \underline{I}_3 \\ \underline{I}_4 \end{bmatrix} \quad \text{and} \quad \underline{V} = \begin{bmatrix} \underline{V}_{-B} \\ \underline{V}_1 \\ \underline{V}_2 \\ \underline{V}_3 \\ \underline{V}_4 \end{bmatrix}. \quad \dots(115)$$

In order to solve for the currents we define

$$\begin{aligned} \underline{J}_1 &= \underline{I}_1 + \underline{I}_2 + \underline{I}_3 + \underline{I}_4 \quad \} \\ \underline{J}_2 &= \underline{I}_1 - \underline{I}_2 + \underline{I}_3 - \underline{I}_4 \quad \} \\ \underline{J}_3 &= \underline{I}_1 + \underline{I}_2 - \underline{I}_3 - \underline{I}_4 \quad \} \\ \underline{J}_4 &= \underline{I}_1 - \underline{I}_2 - \underline{I}_3 + \underline{I}_4 \quad \} \end{aligned} \quad \dots(116)$$

and

$$\begin{aligned} \underline{W}_1 &= \underline{V}_1 + \underline{V}_2 + \underline{V}_3 + \underline{V}_4 \quad \} \\ \underline{W}_2 &= \underline{V}_1 - \underline{V}_2 + \underline{V}_3 - \underline{V}_4 \quad \} \\ \underline{W}_3 &= \underline{V}_1 + \underline{V}_2 - \underline{V}_3 - \underline{V}_4 \quad \} \\ \underline{W}_4 &= \underline{V}_1 - \underline{V}_2 - \underline{V}_3 + \underline{V}_4 \quad \} \end{aligned} \quad \dots(117)$$

and also

$$\begin{aligned} U_1 &= Z_1 + Z_2 + Z_3 + Z_4 \quad \} \\ U_2 &= Z_1 - Z_2 + Z_3 - Z_4 \quad \} \\ U_3 &= Z_1 + Z_2 - Z_3 - Z_4 \quad \} \\ U_4 &= Z_1 - Z_2 - Z_3 + Z_4 \quad \} \end{aligned} \quad \dots(118)$$

We now solve the equivalent equations

$$U_i \underline{J}_i = \underline{W}_i, \quad i = 2, 3, 4 \quad \dots(119)$$

$$\text{and} \quad \begin{bmatrix} \frac{1}{4} Z_B & Z_A^T \\ Z_A & U_1 \end{bmatrix} \begin{bmatrix} 4\underline{I}_B \\ \underline{J}_1 \end{bmatrix} = \begin{bmatrix} \underline{V}_B \\ \underline{W}_1 \end{bmatrix}. \quad \dots(120)$$

Lastly, we obtain the currents from the transformations

$$\begin{aligned} \underline{I}_1 &= \frac{1}{4} (\underline{J}_1 + \underline{J}_2 + \underline{J}_3 + \underline{J}_4) \} \\ \underline{I}_2 &= \frac{1}{4} (\underline{J}_1 - \underline{J}_2 + \underline{J}_3 - \underline{J}_4) \} \\ \underline{I}_3 &= \frac{1}{4} (\underline{J}_1 + \underline{J}_2 - \underline{J}_3 - \underline{J}_4) \} \\ \underline{I}_4 &= \frac{1}{4} (\underline{J}_1 - \underline{J}_2 - \underline{J}_3 + \underline{J}_4). \} \end{aligned} \quad \dots(121)$$

Once again we note that U_1 , U_2 , U_3 and U_4 are all symmetric as is the matrix in equation (120). This can be taken advantage of to reduce storage requirements and allows the Harwell routine MA29 to be used for all the factorizations.

The major programming difficulty in both sections 7.2 and 7.3 will come in the geometry package, in setting up the correct overlaps for wires crossing symmetry planes and in adding in the correct contributions to finite conductivity - this latter is probably the most difficult but it is anticipated that much of the programming provided for the rotational symmetry option in section 7.1 will carry over in a straightforward manner. If two wires meet at the symmetry plane, then the overlap will need to be put in the matrix Z_A , unless there are three segments under the triangle function on one side of the symmetry plane and one segment on the other. When more than two wires meet, then to obtain a symmetric set of overlaps, it will be necessary for one of these wires to lie in the symmetry plane.

8. SPARSE MATRIX APPROXIMATION

Inevitably there are problems which require matrices too large to fit into the computer. One scheme for reducing the storage needed for bodies a few wavelengths long is to approximate the full matrix by a sparse matrix by neglecting interactions between parts of the body which are more than a certain distance apart.

A special sparse matrix version of CHAOS has been written incorporating this idea. It uses the Harwell routine MA28 [13], modified for complex arithmetic, to factorize the impedance matrix, Z , into the sparse factors which are upper, U , and lower, L , triangular. Thus, we have

$$Z = L.U. \quad \dots(122)$$

Unfortunately, there is no reliable routine available to produce a symmetric factorization of Z although Harwell are expecting to produce one in due course (it is provisionally named MA27). This has the consequence that more storage is used than is necessary. Also it has been noticed that in the L and U factors, there are many small elements which can be neglected without significantly affecting the radar cross-sections. Now, because the factorization is unsymmetric, the dropping of these small elements breaks the symmetry and so the principle of reciprocity is not exactly satisfied. So there are at least two compelling reasons for changing to a symmetric factorization routine as soon as possible.

9. COMPLEX FREQUENCY VERSION OF CHAOS

Let us consider the equation (29) which may be written symbolically as

$$\underline{Z}\underline{I} = \underline{V}, \quad \dots(123)$$

where Z is the known impedance matrix, \underline{V} is the known voltage vector and \underline{I} is the unknown current vector. Now the complex frequencies, S_i , at which the determinant of Z is zero are given by

$$\det Z(S_i) = 0. \quad \dots(124)$$

The current, for some complex frequency S , may be expanded as

$$\underline{I}(S) = \sum_{i=1}^{\infty} \frac{1}{(S - S_i)} \underline{R}_i. \quad \dots(125)$$

In the time domain, we have the Fourier transform

$$\underline{I}(t) = \sum_{i=1}^{\infty} e^{S_i t} \underline{R}_i. \quad \dots(126)$$

So the S_i establish the resonance frequencies and the decay times of the structure and depend on the structure only. They are independent of polarisation and orientation of the structure. However, the amplitudes \underline{R}_i are dependent on polarisation, orientation and structure, but not on frequency. This scheme is known as the singularity expansion method [14] and is abbreviated to SEM in the literature.

Each structure is thought to have a unique set of S_i but it requires a considerable amount of computing time to calculate each S_i . The \underline{R}_i may be calculated rather more easily once the S_i are known. In certain circumstances, the S_i can be extracted from experimental measurements of the time dependent response of a structure to a Gaussian or wide band pulse.

The CHAOS program has been modified to calculate the complex resonant frequencies S_i . It uses a search procedure in the complex frequency plane due to Muller [15]. This method essentially takes three guesses to a zero and fits a parabola through the values of the determinant of the corresponding impedance matrices. The next approximation to the zero is found as a zero of this parabola. The first guess is then discarded and the approximation just found is substituted. The process is then repeated until convergence. However, this scheme is not a very efficient one as it can fail to find some zeroes and has difficulties with double zeroes. Its main advantage is that it does not require the derivative of the impedance matrix to be calculated.

How the initial three starting values are chosen needs some explanation. We need to study equations (125) and (126) and remember that we are interested in real solutions to real problems. This implies that the S_i occur in complex conjugate pairs and must lie in the left-hand half of the complex frequency plane in order to produce exponentially decaying currents. For convenience, we choose to work with normalised frequencies and define

$$\bar{S} = \frac{SL}{\pi c}, \quad \dots(127)$$

where c is the velocity of light and L is the maximum linear dimension of the scattering object. With these units our starting guesses for a zero are:-

$$\begin{aligned} \bar{S}^{(1)} &= -0.1 + i0.5 + t, \\ \bar{S}^{(2)} &= -0.15 + t, \\ \bar{S}^{(3)} &= -0.1 + t, \end{aligned} \quad \dots(128)$$

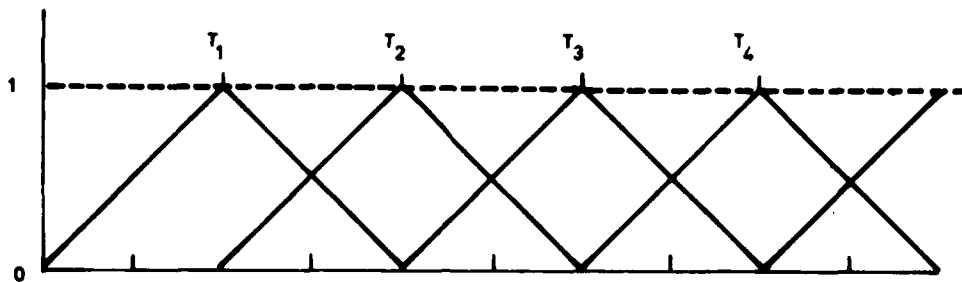
where t may be supplied as data to the program if there is any good reason for knowing what the zero is. If it is not supplied as data, it is taken to be zero. In the case of a dipole one might take t to be $i0.5$, $i1.0$, $i1.5$, etc, corresponding to the known resonances of the dipole. These values have been found by trial and error to be sensible. There is one final problem that needs mentioning; the impedance matrix $Z(S)$ is singular when the frequency is zero. Thus, in the computer program, one works with the combination $SZ(S)$ which is finite at the origin.

A better scheme based on contour integration has been devised by Baum et al. [16]. The idea is to divide the complex frequency plane up into boxes and to evaluate a certain integral around the edge of this box. A set of equations is obtained, one for each integral, which define how many zeroes lie inside the box and provide a set of simultaneous non-linear equations to solve for the required complex frequencies. If there are too many zeroes in the box, it is a trivial task to further subdivide it. The equations that are being used are

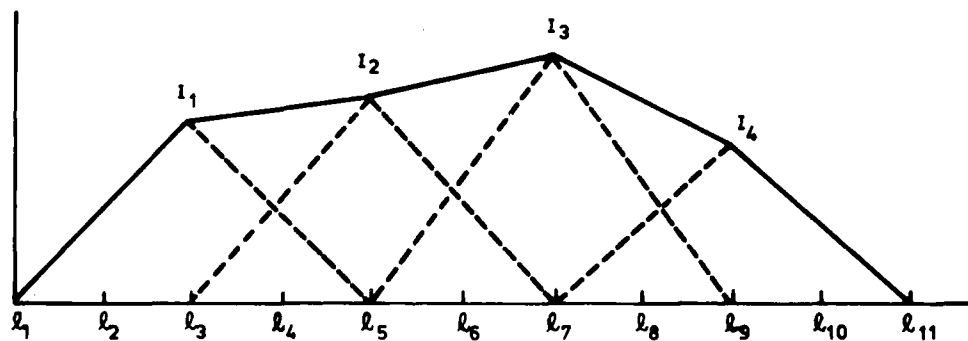
$$\frac{1}{2\pi i} \oint_C S^k \frac{d}{dS} \log Z(S) dS = \sum_{i=1}^M S_i^k, \quad k = 0, 1 \dots M, \quad \dots(129)$$

where M is the number of zeroes inside the contour C . This scheme has not been programmed into CHAOS but should these zeroes be required in future, it would be sensible to change over to Baum's method. It is unlikely to reduce the computing time very much.

(a) TRIANGLE FUNCTIONS



(b) PIECEWISE LINEAR APPROXIMATION TO CURRENT



For $l_{a+1} \leq l \leq l_{2a+3}$

$$\underline{I}(l) = I_a T_{a-a}(l) + I_{a+1} T_{a+1-a+1}(l)$$

$$\sigma(l) = \frac{i}{\omega} \left[I_a \frac{dT_a(l)}{dl} + I_{a+1} \frac{dT_{a+1}(l)}{dl} \right]$$

FIGURE 1

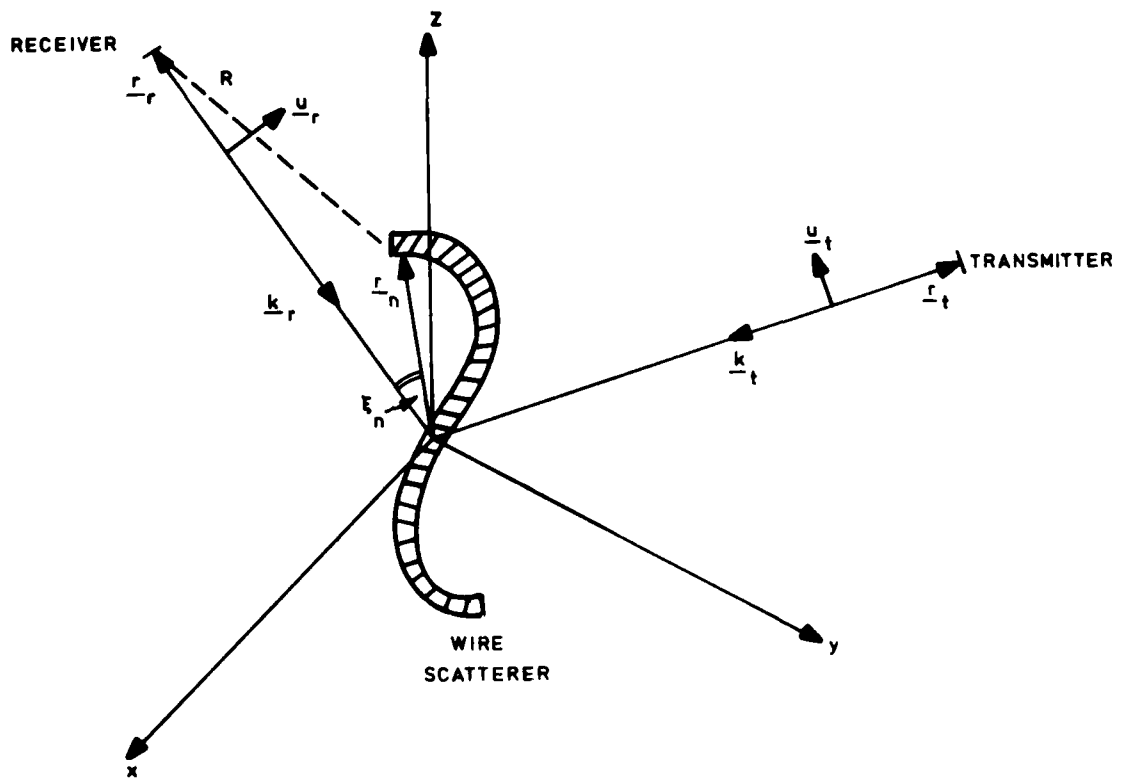
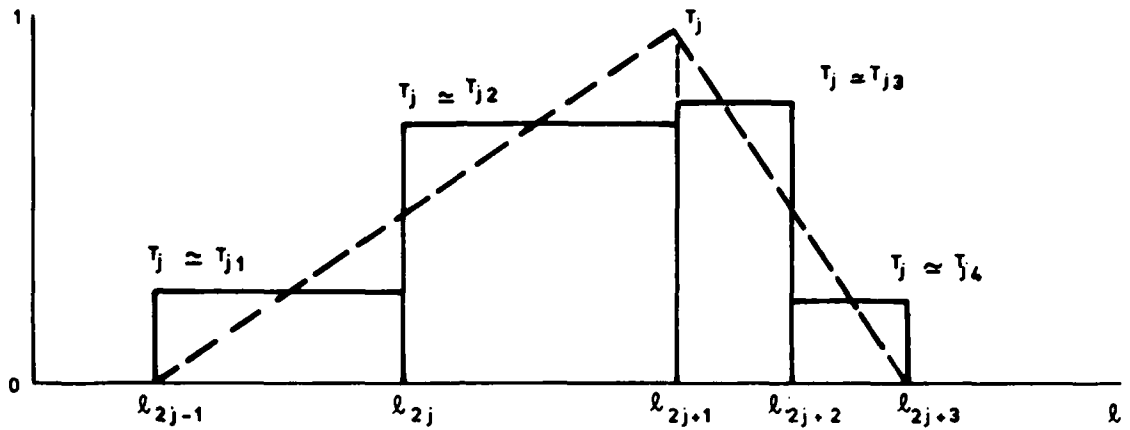


FIGURE 2 Definitions for Plane Wave Scattering

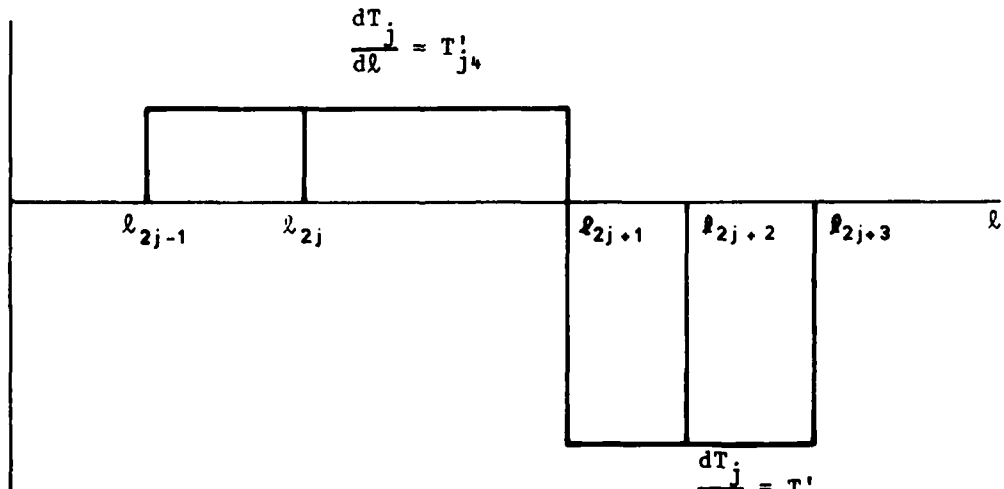
STEP FUNCTION APPROXIMATION TO TRIANGLE FUNCTION T_j



$$T_{j1} = \frac{l_{2j} - l_{2j-1}}{2(l_{2j+1} - l_{2j-1})}, \quad T_{j2} = \frac{1}{2} + T_{j1}$$

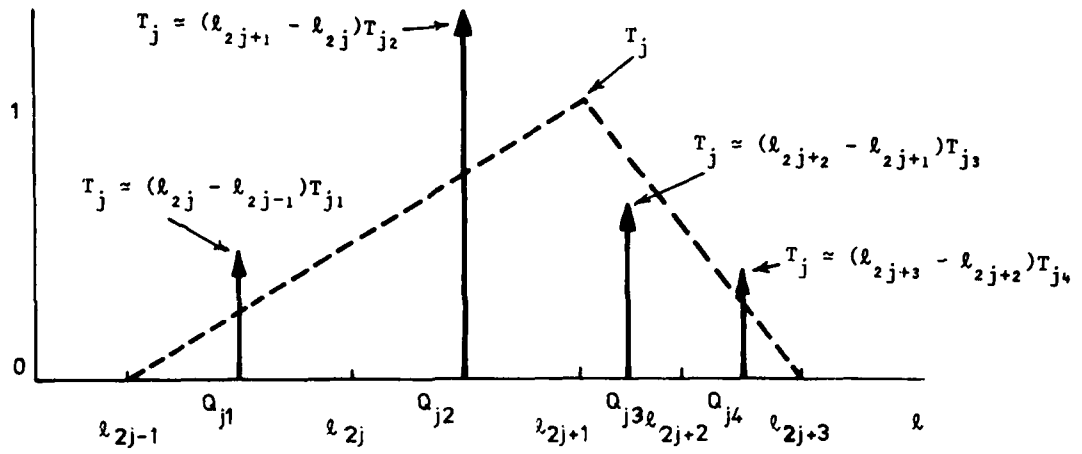
$$T_{j3} = \frac{1}{2} + T_{j4}, \quad T_{j4} = \frac{l_{2j+3} - l_{2j+2}}{2(l_{2j+3} - l_{2j+1})}$$

DERIVATIVE OF TRIANGLE FUNCTION T_j



$$T'_{j1} = T'_{j2} = \frac{1}{l_{2j+1} - l_{2j-1}}, \quad T'_{j3} = T'_{j4} = \frac{-1}{l_{2j+3} - l_{2j+1}}$$

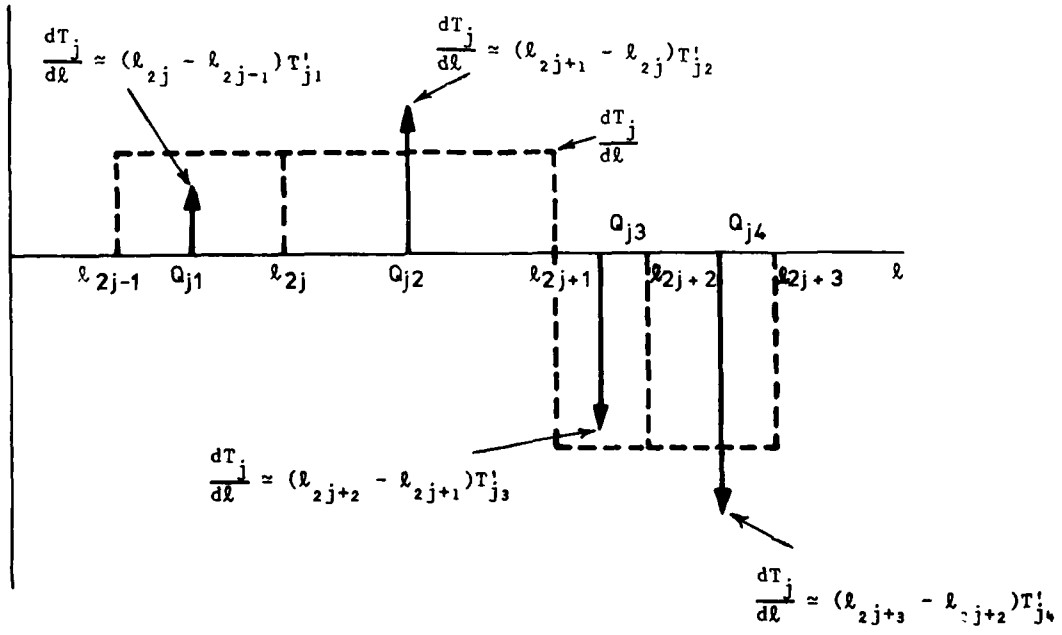
FIGURE 3



$$Q_{ji} = \frac{1}{2} (l_{2j+i-1} + l_{2j+i-2})$$

$$t_{jm} = (l_{2j-1+m} - l_{2j-2+m})T_{jm}$$

IMPULSE APPROXIMATION TO DERIVATIVE OF TRIANGLE FUNCTION T_j



$$t'_{jm} = (l_{2j-1+m} - l_{2j-2+m})T'_{jm}$$

FIGURE 4

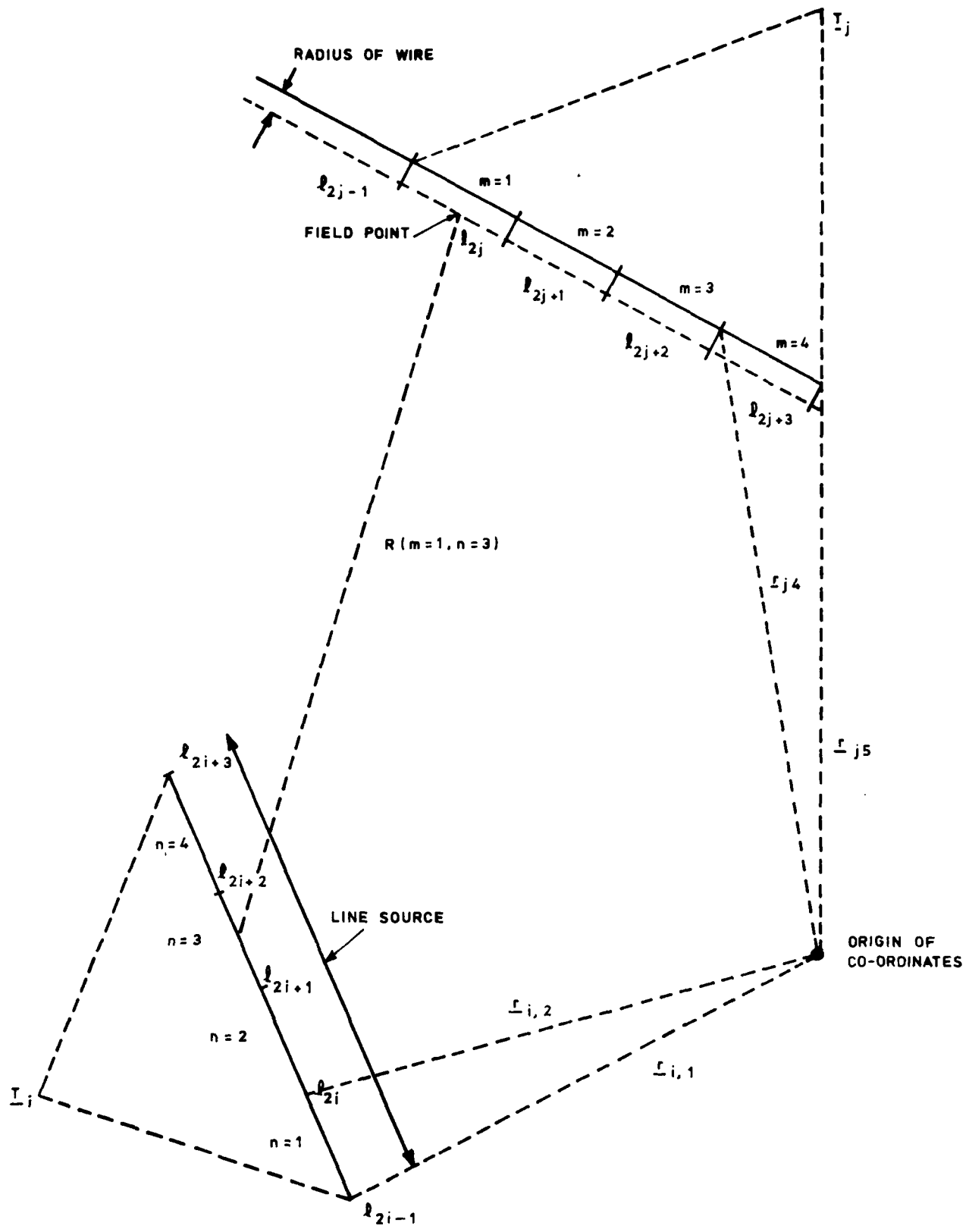
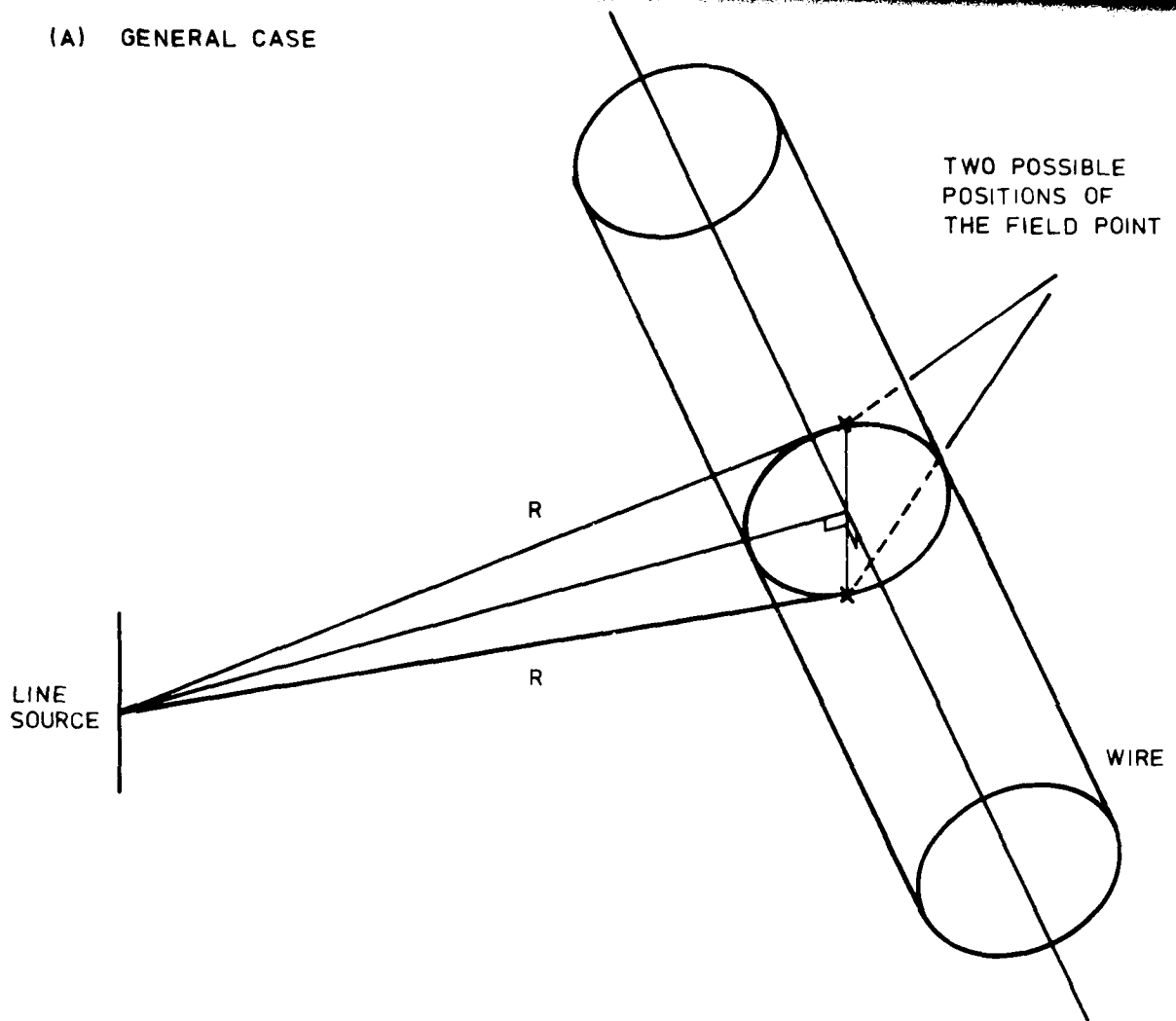


FIGURE 5 Explanation of Notation for Calculation of Interaction between Triangle Functions j and i

(A) GENERAL CASE



(B) DEGENERATE CASE

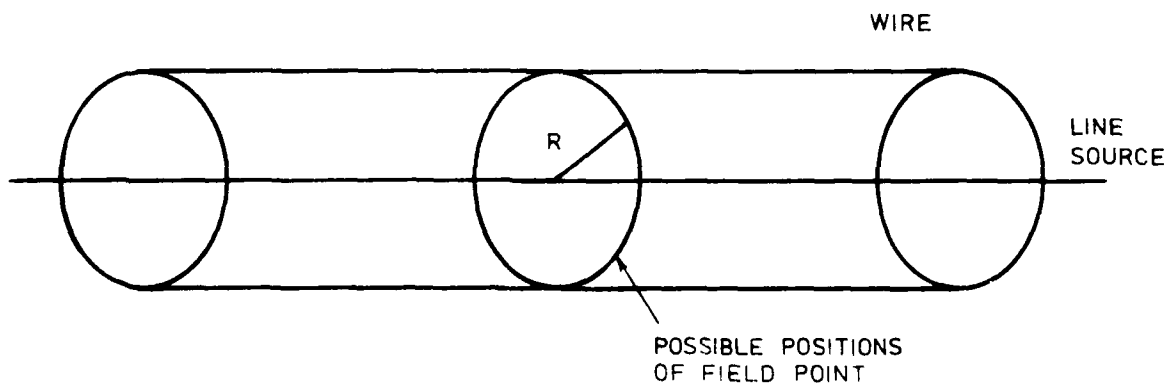
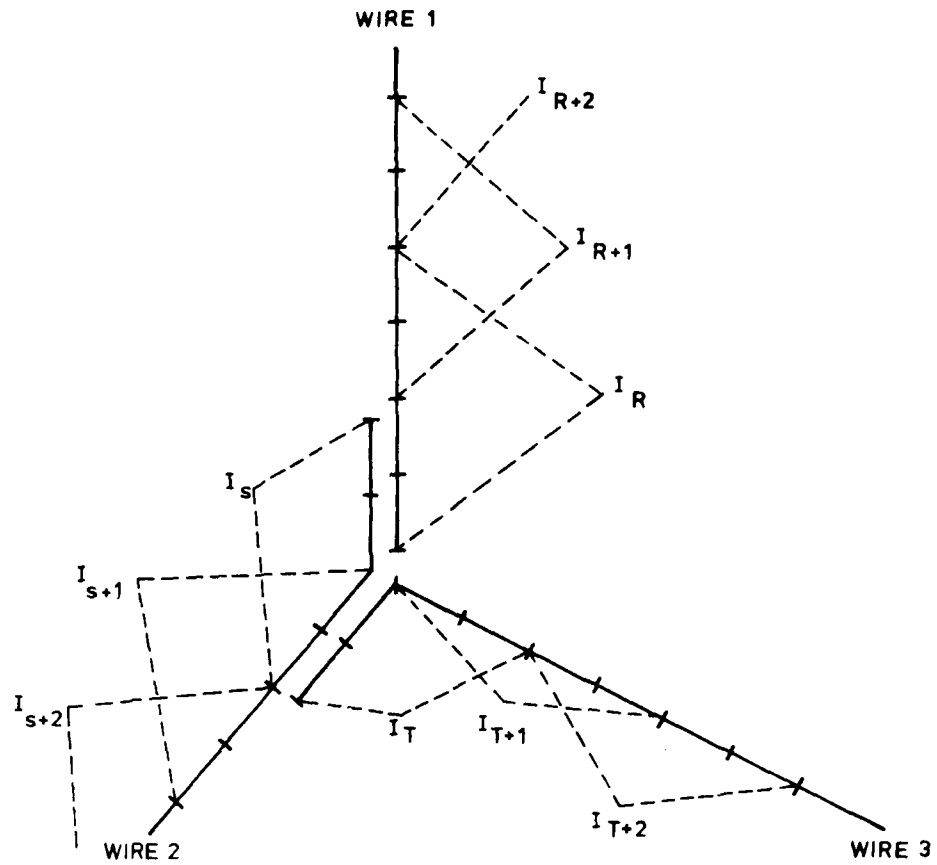
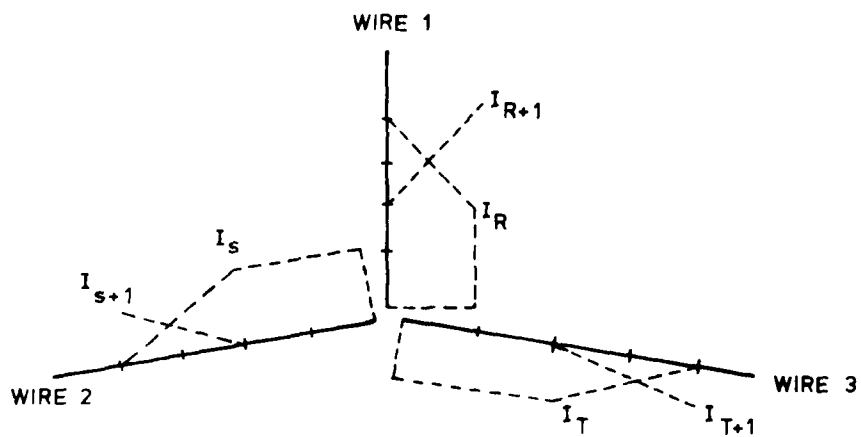


FIGURE 6 Position of the Field Point

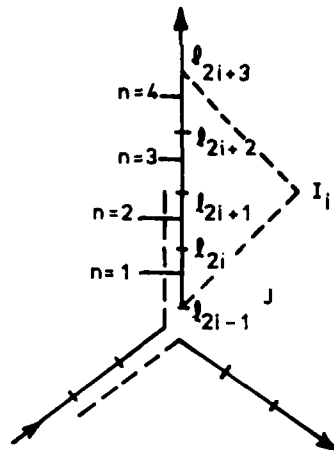


(a) OVERLAPPING WIRE JUNCTION TREATMENT USED BY CHAO AND STRAIT.
(OVERLAPPING TRIANGLE FUNCTIONS SHOWN DASHED.)



(b) JUNCTION TREATMENT WITHOUT OVERLAPS

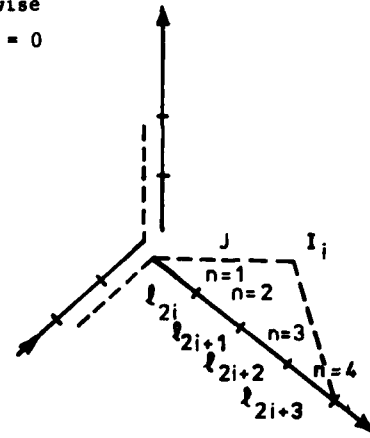
FIGURE 7



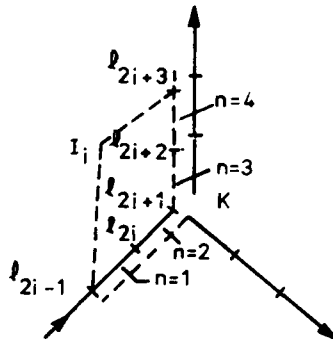
Case (i) $a_i(1) = 0$
 $b_i(1) = 1$

Unless stated otherwise
 $a_i(n) = 1, b_i(n) = 0$

TRIANGLE FUNCTION i
 LEAVES JUNCTION J

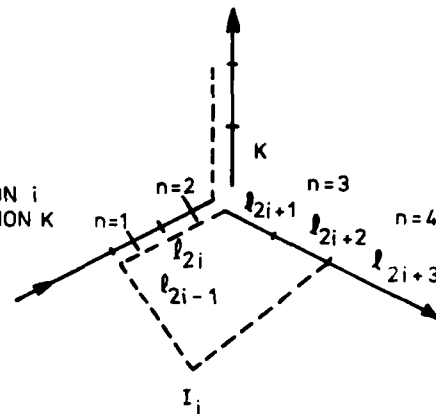


Case (ii) $a_i(1) = 0, b_i(1) = 0,$
 $[a_{i-1}(2) = 0, a_{i-1}(3) = 0, b_{i-1}(3) = 1]$

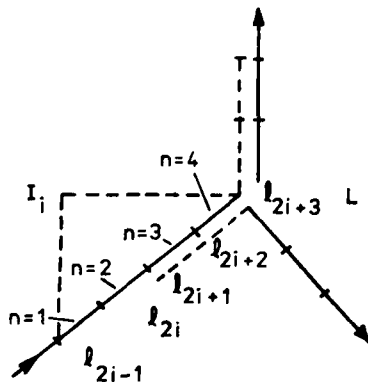


Case (iii) $a_i(2) = 0, a_i(3) = 0,$
 $b_i(2) = 1$
 $[a_{i-1}(4) = 0, b_{i-1}(4) = 0]$

TRIANGLE FUNCTION i
 STRADDLES JUNCTION K

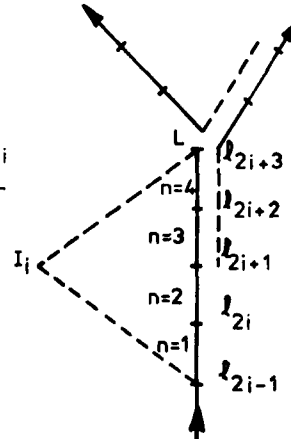


Case (iv) $a_i(2) = 0, a_i(3) = 0,$
 $b_i(3) = 1$
 $[a_{i+1}(1) = 0, b_{i+1}(1) = 0]$



Case (v)
 $a_i(4) = 0, b_i(4) = 0$
 $[a_{i+1}(2) = 0, a_{i+1}(3) = 0, b_{i+1}(2) = 1]$

TRIANGLE FUNCTION i
 ENTERS JUNCTION L



Case (vi)
 $a_i(4) = 0$
 $b_i(4) = 1$

FIGURE 9 Various Situations at a Junction

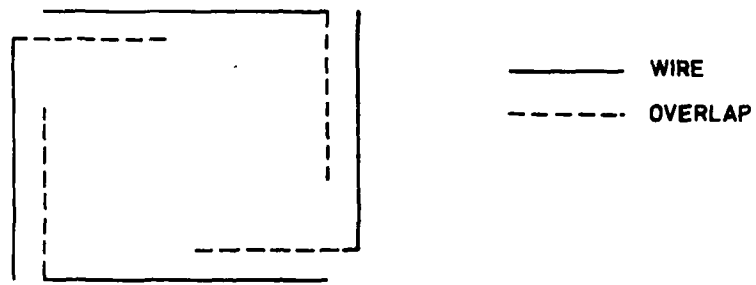


FIGURE 10(a) Illustration of Convention Adopted for Adding Overlaps to a Section to Cause the Whole Structure to be Electrically Connected

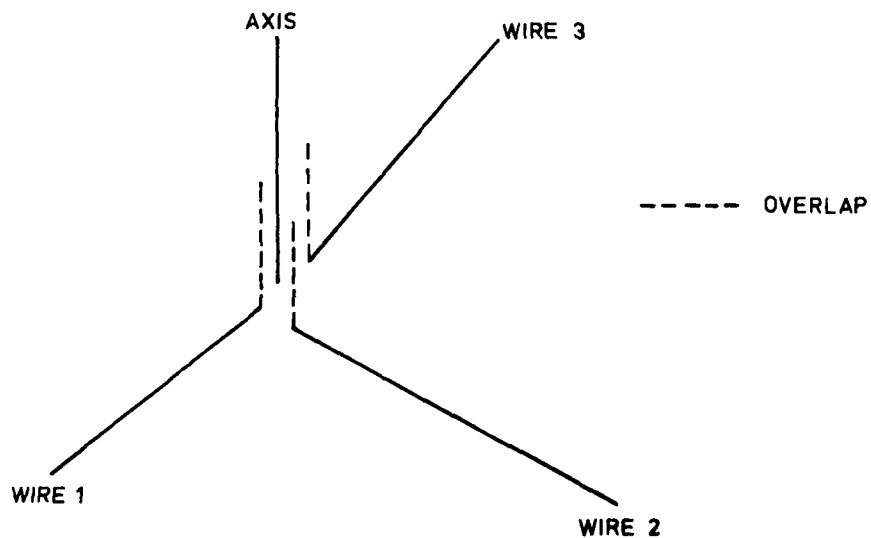


FIGURE 10(b) Illustration of Arrangements of Overlaps Connecting Wires to Axis in a Symmetric Fashion

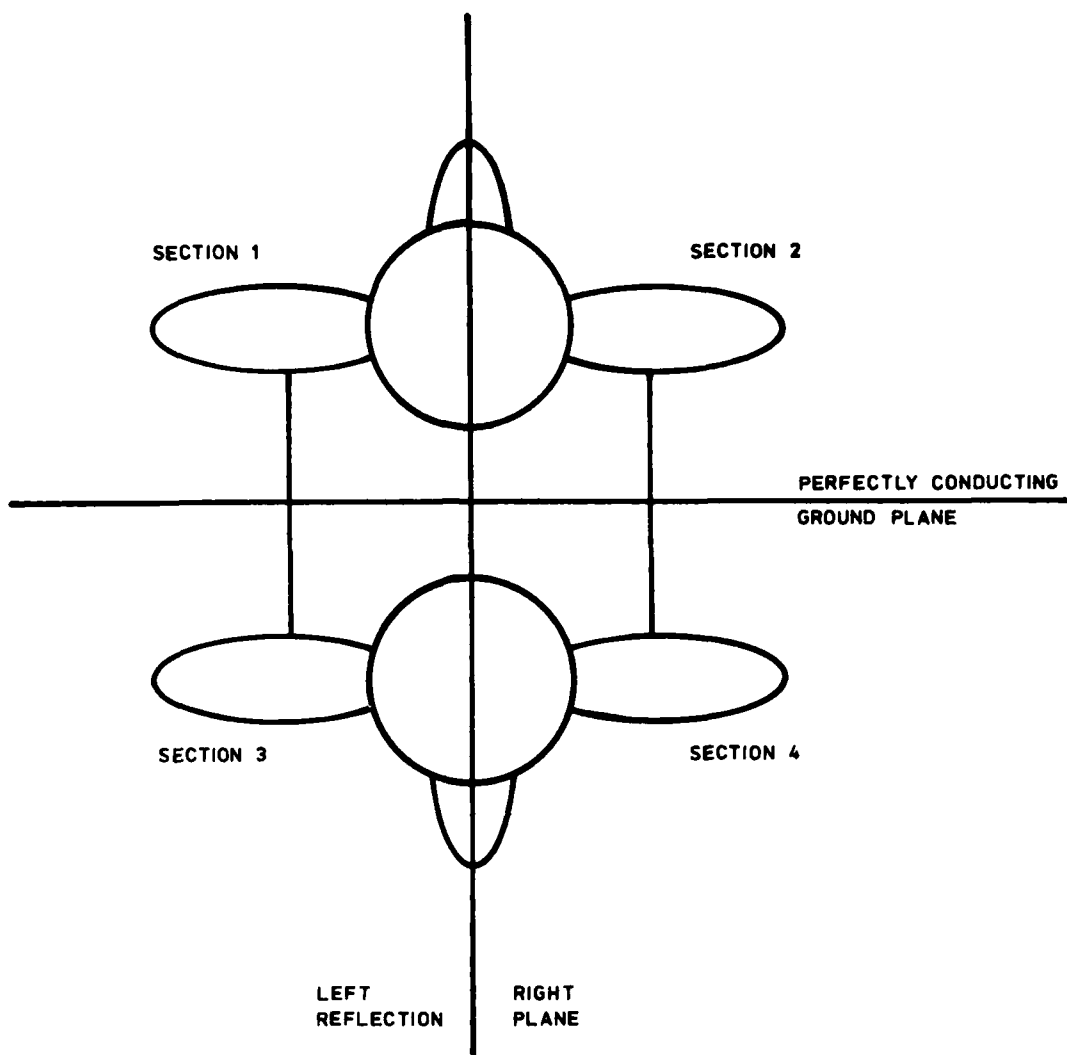


FIGURE 11 Section Numbering Scheme for 2 Planes of Mirror Symmetry

APPENDIX A

ACCURACY

A1. EVALUATION OF ψ FUNCTION

Let us write the ψ function of equation (49) as

$$\psi = \frac{1}{4\pi\Delta} \int_{-\Delta/2}^{\Delta/2} \frac{e^{-ikR}}{R} dz', \quad \dots(A1)$$

where we have chosen a local cylindrical coordinate system based on the source segment as Z axis. The segment length is taken as Δ and the origin of coordinates is at the centre of the segment. Here R is given by

$$R = \sqrt{\rho^2 + (Z - Z')^2}, \quad \dots(A2)$$

where ρ and Z are the cylindrical coordinates of the field point in this system. The geometry is illustrated in figure A1. Since we have stipulated that the field point lies on the wire surface, while the line source lies on the wire axis, the integrand can never become singular.

For $r < 5\Delta$, Harrington recommends the expansion

$$\psi = \frac{e^{-ikr}}{4\pi\Delta} \left[I_1 - ik(I_2 - rI_1) - \frac{k^2}{2} (I_3 - 2rI_2 + r^2I_1) + i \frac{k^3}{6} (I_4 - 3rI_3 + 3r^2I_2 - r^3I_1) \right], \quad \dots(A3)$$

$$\text{where } I_1 = \log \left[\frac{Z + \Delta/2 + \sqrt{\rho^2 + (Z + \Delta/2)^2}}{-Z - \Delta/2 + \sqrt{\rho^2 + (Z - \Delta/2)^2}} \right], \quad \dots(A4)$$

$$I_2 = \Delta, \quad \dots(A5)$$

$$I_3 = \frac{Z + \Delta/2}{2} \sqrt{\rho^2 + (Z + \Delta/2)^2} + \frac{(\Delta/2 - Z)}{2} \sqrt{\rho^2 + (Z - \Delta/2)^2} + \frac{\rho^2}{2} I_1, \quad \dots(A6)$$

$$I_4 = \Delta\rho^2 + 3\Delta^3/12 + \Delta Z^2. \quad \dots(A7)$$

While for $r \geq 5 \Delta$, he recommends

$$\psi = \frac{e^{-ikr}}{4\pi r} \left[A_0 + i \frac{k\Delta}{2} A_1 + \left(\frac{k\Delta}{2}\right)^2 A_2 + i\left(\frac{k\Delta}{2}\right)^3 A_3 + \left(\frac{k\Delta}{2}\right)^4 A_4 \right], \quad \dots (A8)$$

where

$$A_0 = 1 + \frac{1}{6} \left(\frac{\Delta}{2r}\right)^2 \left[-1 + 3\left(\frac{Z}{r}\right)^2 \right] + \frac{1}{40} \left(\frac{\Delta}{2r}\right)^4 \left[3 - 30\left(\frac{Z}{r}\right)^2 + 35\left(\frac{Z}{r}\right)^4 \right], \quad \dots (A9)$$

$$A_1 = \frac{1}{6} \left(\frac{\Delta}{2r}\right) \left[-1 + 3\left(\frac{Z}{r}\right)^2 \right] + \frac{1}{40} \left(\frac{\Delta}{2r}\right)^3 \left[3 - 30\left(\frac{Z}{r}\right)^2 + 35\left(\frac{Z}{r}\right)^4 \right], \quad \dots (A10)$$

$$A_2 = -\frac{1}{6} \left(\frac{Z}{r}\right)^2 - \frac{1}{40} \left(\frac{\Delta}{2r}\right)^2 \left[1 - 12\left(\frac{Z}{r}\right)^2 + 15\left(\frac{Z}{r}\right)^4 \right], \quad \dots (A11)$$

$$A_3 = \frac{1}{60} \left(\frac{\Delta}{2r}\right) \left[3\left(\frac{Z}{r}\right)^2 - 5\left(\frac{Z}{r}\right)^4 \right], \quad \dots (A12)$$

$$A_4 = \frac{1}{120} \left(\frac{Z}{r}\right)^4. \quad \dots (A13)$$

A2. MAXIMUM SEGMENT LENGTH

We next need to know how accurate these formulae are. Both equations (A3) and (A8) are the result of integrating power series expansions term by term and truncating after the fourth and fifth terms respectively. The ratio of the fourth term to the leading term in equation (A3) is $(\pi/N)^3$ and the ratio of the fifth term to the leading term in equation (A8) is $(\pi/N)^4$ where

$$N = \frac{\lambda}{\Delta} = \frac{2\pi}{k\Delta}, \quad \dots (A14)$$

ie, N is the ratio of wavelength to segment length. The use of higher order terms in these expansions has been investigated and, although the accuracy of the impedance matrix elements is improved, the accuracy of the radar cross-sections is less affected for a given value of N. The accuracy of the matrix elements for various values of N is indicated in table A1.

TABLE A1

Percentage Accuracy of Matrix Elements

N	Formula for ψ Function	
	(A3)	(A8)
10	3	1
7	9	4
6	14	8
5	25	16
4	48	38

In CHAOS, the ratio N is printed out for each wire with a warning if it is less than 10. If it is less than 6 for any wire, the job is rejected. Just because the matrix elements are accurate, it does not mean that the current distributions and radar cross-sections are accurate. For simple geometries, like a dipole, one may need as many as 50 segments per wavelength especially if one is near a resonance and wishes to get cross-sections accurate to a few per cent. This is because the frequency at which a dipole resonates, and the cross-section at this frequency, change by about 10% as the number of segments is increased from, say, 10 segments per wavelength to 50. Increasing this figure further leads to only small changes of the order of 1%. However, because the resonance is so narrow, if one is interested in a spot frequency close to the resonance, the cross-section may be wrong by 100% if one uses 10 segments per wavelength. For wires made of material of low conductivity (say, of the order of 10^4 mho/m), for which the resonance effect is not very pronounced, fewer segments are necessary.

For complicated geometries, it appears that one can get away with 14 segments per wire for good conductors and 10 segments per wire for other materials. This should give the positions of lobes in the radar cross-section pattern correct to about $\pm 5^\circ$ and the amplitudes of the largest lobes correct to about ± 2 db. It is not possible to be more precise because of the impossibility of using shorter segments due to

computer storage limitations and because more accurate experimental data on complicated geometries does not appear to be available.

It is up to the user to satisfy himself that his calculations are properly converged by staging calculations with more segments where possible, checking against whatever experimental data he may have and using his common sense.

A3. SMALL SEGMENT LENGTHS

Intuitively, one would expect to get a better and better answer to a calculation as the segment length is reduced. This is not found to be the case and needs explanation. Let us consider a straight dipole of length L and evaluate the matrix elements given by equation (32) in the limit as Δ the segment length tends to zero keeping the wavelength and radius fixed. We find after some manipulation that

$$Z_{ji} = \frac{l_{ji}}{8} Z_{\omega} \Delta + \frac{e^{-ikr_p}}{\pi r_p} \left[i\omega\mu - \frac{(3 + 3ikr_p - k^2 r_p^2)}{i\omega\epsilon r_p^2} \left(\frac{p\Delta}{r_p} \right)^2 \right] \Delta^2, \quad \dots(A15)$$

where

$$l_{ji} = \begin{cases} 10 & \text{if } j = i, \\ 3 & \text{if } j = i \pm 1, \\ 0 & \text{otherwise,} \end{cases}$$

$$p = 2(j - i),$$

$$r_p = \sqrt{a^2 + p^2 \Delta^2}.$$

The matrix order for such a problem is $(L/2\Delta) - 1$. The structure of this impedance matrix is curious. The main diagonals and the diagonals on either side of it are of the order of Δ for very small segment lengths while all other terms are of the order of Δ^2 . In any one row of this matrix there are roughly $L/2\Delta$ elements of the order of Δ^2 , so that these could add up to give a term of the order of Δ which would then be comparable to the diagonal term. It has been found that when a 32 bit computer word length is used problems start to arise if there are 1000 or more segments on a wire. Thus, the CHAOS program will reject all problems which contain any wire divided into more than 500 segments.

Let us now recall what is happening physically to our segment as this limit is approached. It starts out being in the form of a long thin cylinder and changes through a short fat cylinder to eventually become a wafer thin disc. The formulae used in CHAOS are based on the assumption of a long thin cylinder and we need to know how short the cylinder can become before this assumption is violated. Let us define the aspect ratio R to be the ratio of segment length to radius. From numerical experiments with CHAOS using a dipole, we find that when R is as small as 0.1, the current distributions become highly oscillatory with spatial period 2Δ . These current distributions appear to be all right for R equal to 0.5. Thus, we have decided to reject all jobs for which R is less than 0.5 but warning messages are printed out if R is less than 5.

A4. ANOTHER LIMITING CASE

Another limiting case which is of interest is that which occurs when the segment length Δ tends to zero in such a way that the ratio of segment length to radius, R , remains constant at the same large value. After some further manipulation we find the impedance matrix elements to be:-

$$Z_{jj} = \frac{-1}{4\pi\omega\epsilon\Delta} \left[2 \log \frac{\Delta}{a} - \frac{1}{6} \right] + \frac{5}{4} Z_{\omega\Delta} + O(k\Delta), \quad \dots(A16)$$

$$Z_{j,j\pm 1} = \frac{i}{4\pi\omega\epsilon\Delta} \left[\log \frac{\Delta}{a} - \frac{49}{120} \right] + \frac{3}{8} Z_{\omega\Delta} + O(k\Delta), \quad \dots(A17)$$

$$Z_{j,i} = \frac{iqe^{-iq\Delta}}{4\pi\omega\epsilon\Delta} \left[-\frac{1}{q^2} - \frac{1}{2(q^2-1)} + \frac{1}{q^2-4} + \frac{1}{2(q^2-9)} \right. \\ \left. + ik\Delta \left\{ -\frac{1}{2(q^2-1)} + \frac{4}{q^2-4} + \frac{9}{2(q^2-9)} \right\} \right] + O(k\Delta), \quad \dots(A18)$$

where $i \neq j$, $j \pm 1$ and $q = 2|j - i|$.

Suppose now we restrict our dipole to have four segments and to be a perfect conductor, then the radar cross-section will be

$$\sigma_{\theta\theta}(\theta) = \frac{\pi k^4 L^6 \sin^4 \theta}{256 \left(\log \frac{L}{4a} - \frac{1}{12} \right)^2}, \quad \dots(A19)$$

$$\sigma_{\theta\phi}(\theta) = 0, \quad \sigma_{\phi\phi}(\theta) = 0$$

where $L = 4\Delta$ and θ is the angle between the direction of the transmitter/receiver and the axis of the dipole. ϕ is the azimuthal angle about this axis. The notation $\sigma_{\theta\phi}$ means the radar cross-section for the transmitter polarised in the direction of increasing θ , while the receiver is polarised in the direction of increasing ϕ .

From the book by Ruck [17], the radar cross-section for a perfectly conducting short thin cylinder of length L and radius a is

$$\sigma_{\theta\theta}(\theta) = \frac{\pi k^4 L^6 \sin^4 \theta}{144 \left(\log \frac{2L}{a} - 1\right)^2}, \quad \dots(A20)$$

$$\sigma_{\theta\phi}(\theta) = 0, \quad \sigma_{\phi\phi}(\theta) = 0.$$

These two sets of formulae are not quite the same and reflect the fact that in CHAOS the current distribution is forced to be triangular in shape while the formulae given by Ruck are obtained by treating the dipole as the limiting case of a prolate spheroid. These are only equal when L/a is about 157 and for larger values of L/a the CHAOS prediction will be smaller than those of Ruck.

A5. PROBLEMS AT VERY LOW FREQUENCIES

The behaviour of the impedance matrix as the frequency tends to zero is yet another interesting limit. In this case we can expand e^{-ikR} in equation (45) as

$$e^{-ikR} \approx 1 - ikR + O(k^2), \quad \dots(A21)$$

since kR is small compared to 1 when the frequency is so low that the largest dimension of the scattering body is much smaller than the wavelength. Thus,

$$Z_{ji}^E = \frac{1}{4\pi i \omega \epsilon} \int_{\text{wires}} d\ell \int_{\text{wires}} d\ell' \frac{1}{R} \frac{d}{d\ell} T_j(\ell) \frac{d}{d\ell'} T_i(\ell') + O(k), \quad \dots(A22)$$

where the term of order unity integrates to zero.

From equation (44) we also have

$$Z_{ji}^M = 0(k), \quad \dots(A23)$$

while from equation (47) using equations (78) and (79) we have

$$Z_{ji}^C = 0(1). \quad \dots(A24)$$

Thus, the imaginary part of the impedance matrix Z_{ji} is $0(1/k)$ while the real part is $0(1)$ for non-perfect conductors and $0(k)$ for perfect conductors. So we can split the matrix into three parts as

$$Z_{ji} = R_{ji} + iL_{ji} + T_{ji}, \quad \dots(A25)$$

where

$$R_{ji} = 0(k),$$
$$L_{ji} = 0\left(\frac{1}{k}\right),$$
$$T_{ji} = 0(1).$$

We wish to solve

$$(R + iL + T)\underline{I} = \underline{V}, \quad \dots(A26)$$

where $V_j = 0(1)$ as $k \rightarrow 0$, for the currents I_i . In general this should present no problems and at low frequency is equivalent to solving

$$iL\underline{I} = \underline{V} \quad \dots(A27)$$

to give currents of $0(k)$ which is intuitively sensible since at low frequency, the whole structure is at the same potential and no currents will flow. The trouble comes for those structures for which the determinant of L is singular, as in the case of a planar loop of wire. For this case equation (A27) has many solutions and for a given finite computer word length there is a frequency below which the problem cannot be solved.

Thus, a test has been programmed into CHAOS to detect the situation where the matrix Z is nearly singular. This is done by examining the factorized form of Z , be it LDL^T (for symmetric matrices) or LU (for unsymmetric cases). The maximum and minimum elements of the diagonals of either D or U are found and the ratio is taken. From tests on a dipole, it has been found that when this ratio is greater than 25000 for a computer word length of 32 bits, the results will be spurious. In CHAOS, if the ratio exceeds 20000 the calculation is terminated and no results can be obtained. In cases where this ratio is only just less than 20000 (the maximum and minimum are printed out by the program), results should be checked to see that they are intuitively sensible. For computers which use a 64 bit word length, the results appear to be sensible for values of this ratio up to 100000; beyond this value they progressively deteriorate.

A6. COMPUTER WORD LENGTH PROBLEMS

The CHAOS program has been made to work on both an IBM computer using 32 bit word length and a CRAY computer using 64 bit word length. Tests have been carried out on both machines using a matrix of order 650. In general, no significant change in results has been noticed. In particular, at and near the peaks of a radar lobar diagram, there is usually no change to four significant figures although occasionally a change of one unit in the fourth figure does occur. In the troughs between the lobes, the changes can be, and are, much bigger and radar cross-sections which are six orders of magnitude smaller than the maximum using 32 bit word length can become fourteen orders of magnitude smaller using a 64 bit word length. However, these are large changes in small and insignificant numbers and so are of no consequence.

The only other change is that, as already mentioned at the end of the previous section, the use of a longer word length allows calculations to be done at slightly lower frequencies than can be done with a 32 bit word length.

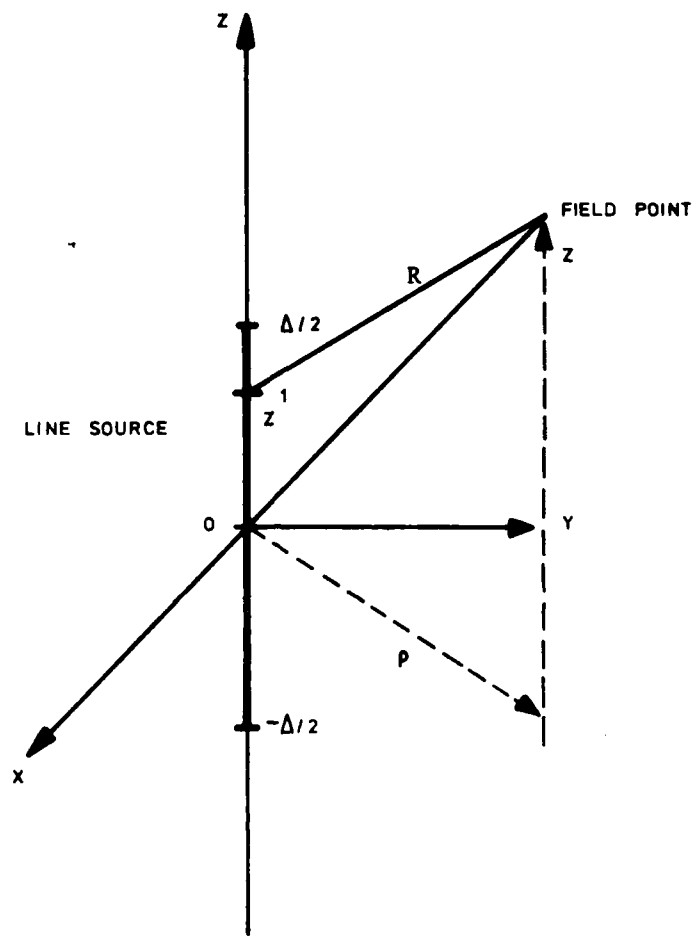


FIGURE A1 Geometry for Calculating ψ Function

APPENDIX B

CONVENTIONS USED IN CHAOS

B1. INTRODUCTION

This appendix details the time and phase conventions, together with the coordinate systems that may be used to describe the effect of an electromagnetic wave being scattered by a body. The system as described here is used in the CHAOS computer program.

B2. WHY USE A COMPLEX REPRESENTATION FOR A REAL EFFECT?

The first point to explain is why, when we are dealing with real electric fields and real currents in a real world, we should represent these by complex quantities. The short answer is that this is mathematically convenient as may be seen by studying the structure of Maxwell's equations for the electromagnetic fields.

From equations (1), (3) and (58), it may be seen that

$$\nabla \cdot \nabla \cdot \underline{\underline{E}} + \mu\sigma \frac{\partial}{\partial t} \underline{\underline{E}} + \mu\epsilon \frac{\partial^2}{\partial t^2} \underline{\underline{E}} = 0, \quad \dots(B1)$$

where ϵ , μ , and σ are assumed to be constant and $\underline{\underline{E}}$ is the real electric field. Equation (B1) can be further simplified by assuming a cosinusoidal time variation at a constant frequency ω . We could write all quantities in the form

$$\underline{\underline{E}}_j(\underline{\underline{r}}, t) = A_j(\underline{\underline{r}}) \cos(\omega t + \phi_j) \text{ for } j = x, y, z, \quad \dots(B2)$$

but substitution into equation (B1) then gives an inelegant and rather cumbersome equation to solve. It is much more convenient mathematically to write

$$\underline{\underline{E}}(\underline{\underline{r}}, t) = \underline{\underline{E}}(\underline{\underline{r}}) e^{i\omega t}, \quad \dots(B3)$$

where $\underline{E}_j(\underline{r}) = A_j(\underline{r})e^{i\phi_j}$ for $j = x, y, z,$ (B4)

and then to solve $\nabla \cdot \nabla \underline{E}(\underline{r}) - T^2 \underline{E}(\underline{r}) = 0,$ (B5)

where $T^2 = -i\omega\mu(\sigma + i\omega\epsilon).$ (B6)

Once we have the solution to the complex equation (B5) it is a trivial job to obtain the solution (B2) to the real problem.

B3. TIME CONVENTION AND COORDINATE SYSTEM

Following the discussion of section B2 the time variation will be described by $e^{i\omega t}$, where ω is the frequency in radians/second. The complex time dependent electric field is defined as

$$\underline{E}(\underline{r}, t) = \underline{E}(\underline{r})e^{i\omega t}. \quad \dots(B7)$$

The real time dependent electric field is given by

$$\underline{\mathcal{E}}(\underline{r}, t) = \text{Re}\underline{E}(\underline{r}, t). \quad \dots(B8)$$

When a radar looks at an object, there are in general two coordinate systems which are of interest. The first is a system fixed with respect to the object as used in the computer program CHAOS. In this system the Z axis, of a right-handed cartesian system OXYZ, might for instance be chosen to be the axis about which the body has some natural symmetry. In this system the radar beam would be incident from a direction defined by (θ, ϕ) , the usual spherical coordinates (see figure B1(a)). Thus, the incident electric field transverse to the direction of propagation would have components in the θ and ϕ directions.

The second system of coordinates is fixed with respect to the radar and is again a right-handed cartesian coordinate system Oxyz in which the radar wave propagates along the z axis from large positive z towards $z = 0$. It is convenient to take the x axis in the direction of increasing θ , and y in the

direction of increasing ϕ , where these directions are as defined in the first system. In figure B1, these axes are offset along the radar line of sight for clarity. In the program CHAOS, it is assumed that the object axis (OZ) is vertical so that the y axis is necessarily horizontal. The x axis then forms the third member of an orthogonal triad. Conventionally (as in the nomenclature "VV polarisation") the x axis is referred to as "vertical" though this is a misnomer unless the radar line of sight lies in the horizontal plane. For this special case (figure B1(b)) Ox is truly vertical, actually vertically downwards. It would be more sensible if CHAOS print outs used the phrase θ and ϕ polarisation in place of vertical and horizontal polarisation.

In the radar coordinate system, a typical complex electric wave, travelling inwards from large z towards $z = 0$ along the z axis, would be represented by

$$\underline{E}(r) = (A_x e^{i(kz+\phi_x)}, A_y e^{i(kz+\phi_y)}, 0), \quad \dots(B9)$$

where $k = 2\pi/\lambda$ is the wave number, $\lambda = 2\pi c/\omega$ is the wavelength and c is the velocity of light. The sign of z is changed for a wave travelling outwards from $z = 0$ to large positive z. The phases ϕ_x and ϕ_y are related to the time origin and only the phase difference is of any physical significance. The two amplitudes A_x and A_y could be replaced by an amplitude $\sqrt{A_x^2 + A_y^2}$ times the appropriate cosine or sine of some angle; however, it is simpler to treat them in this way.

B4. POLARISATION CONVENTIONS

The real time dependent electric field is

$$\underline{E}(r,t) = \text{Re}(A_x e^{i(\omega t+kz+\phi_x)}, A_y e^{i(\omega t+kz+\phi_y)}, 0). \quad \dots(B10)$$

This vector lies in the xy plane and is in general rotating about the z axis. The angle that \underline{E} makes with the x axis is Ψ where

$$\tan \Psi = \frac{A_y \cos(\omega t + kz + \phi_y)}{A_x \cos(\omega t + kz + \phi_x)}. \quad \dots(B11)$$

The magnitude of $\underline{\mathcal{E}}$ is

$$|\underline{\mathcal{E}}| = \sqrt{A_x^2 \cos^2 (\omega t + kz + \phi_x) + A_y^2 \cos^2 (\omega t + kz + \phi_y)}. \quad \dots(B12)$$

For linear polarisation Ψ is, by definition, constant. Since

$$\frac{d\Psi}{d\omega t} = \frac{A_x A_y \sin (\phi_x - \phi_y)}{|\underline{\mathcal{E}}|^2} \quad \dots(B13)$$

in general this implies $\phi_x - \phi_y = n\pi$, where n is any integer. The electric vector therefore makes a constant angle $\pm \tan^{-1} (A_y/A_x)$ with the x axis. The other two possible solutions to equation (B13) are $A_y = 0$ (vertical polarisation) and $A_x = 0$ (horizontal polarisation) and these are also just special cases of the general solution.

If $\phi_x < \phi_y$ and A_x and A_y have the same sign, then Ψ decreases as time increases and elliptic polarisation in a clockwise (right-hand) direction about the direction of propagation and looking along the direction of propagation is obtained* (see figure B2). The polarisation is elliptic because the magnitude of the electric field given by equation (B12) traces out an ellipse in the xy plane.

In order to obtain circular polarisation the magnitude of $\underline{\mathcal{E}}$ must be independent of time. For this to occur, A_x must equal A_y and $\phi_y = \phi_x + (2n \pm 1)\pi/2$ where n is any integer.

It is also instructive to ask what shape the beam has at some fixed instant of time.

For t constant,

$$\frac{d\Psi}{d(kz)} = \frac{A_y \sin (\phi_x - \phi_y)}{A_x \cos^2 (\omega t + kz + \phi_x)}. \quad \dots(B14)$$

If $\phi_x < \phi_y$ and A_x and A_y have same sign, then Ψ decreases as one moves along the wave (from large z to small z) in the direction of propagation, so that a left-hand "corkscrew" is obtained. Thus, this left-handed (anti-clockwise) "corkscrew" in space moves forward and rotates in a right-handed (clockwise) direction as time increases when looking in the direction of propagation.

*This is the right-hand thread rule referred to the direction of propagation which agrees with the definitions of the IRE 1942 standards [18].

B5. INCIDENT AND SCATTERED FIELDS

The incident field will be assumed to be a plane wave of the type given by equation (B8). This will be correct provided the transmitter is sufficiently far from the scattering obstacle.

Using the asymptotic form for the scattered field, it can be shown that the field transverse to the direction of propagation is $O(1/r)$ where r is the distance of the field point from the scatterer while the field in the direction of propagation is $O(1/r^2)$. So at large distances from the scatterer the field becomes essentially transverse to its direction of propagation. The behaviour of the components of the field determine the polarisation of the scattered wave. The polarisation of the receiver will determine which of these components, if any, is measured.

B6. SCATTERING MATRIX

An incident elliptically polarised field $\underline{E}^i(\underline{r})$ can be expressed in terms of cartesian coordinates (as shown in section B3) and so may be related to cartesian coordinates of the backscattered field $\underline{E}^s(\underline{r})$ by a scattering matrix [19], S , where

$$\underline{E}^s(\underline{r}) = S \underline{E}^i(\underline{r}). \quad \dots(B15)$$

Having found the scattering matrix, S , for a given pair of orthogonally polarised fields, it is convenient to be able to transform this matrix to S^1 , where S^1 refers to a different pair of orthogonally polarised fields (eg, S might refer to linearly polarised fields in the θ and ϕ directions and S^1 to circularly polarised fields with left- and right-handed rotations about the direction of propagation). This may be done by means of a change of polarisation basis and the fields may be expressed in terms of an elliptic basis instead of a linear one by a coordinate transformation U .

Now equation (B9) may be re-written as

$$\underline{E}(\underline{r}) = E_{\theta} \underline{u}_{-x} + E_{\phi} \underline{u}_{-y}, \quad \dots(B16)$$

where \underline{u}_x and \underline{u}_y are unit vectors in the x (or θ) and y (or ϕ) directions. Suppose \underline{u}_ξ and \underline{u}_η are an arbitrary pair of orthogonal vectors coplanar with \underline{u}_x and \underline{u}_y , then they must be obtained from them by a unitary transformation. In this case the matrix U has the property that

$$U^{*T}U = I, \quad \dots(B17)$$

where T denotes transpose and * denotes complex conjugate.

So the incident electric field in the elliptic basis, $\underline{\xi}^i$, is given by

$$\underline{\xi}^i = U\underline{E}^i(\underline{r}). \quad \dots(B18)$$

Then
$$\underline{E}^s(\underline{r}) = SU^{-1}U\underline{E}^i(\underline{r}) = SU^{-1}\underline{\xi}^i. \quad \dots(B19)$$

The scattered field is transformed by the same transformation so that

$$\underline{\xi}^s = U\underline{E}^s(\underline{r}) = USU^{-1}\underline{\xi}^i, \quad \dots(B20)$$

where $\underline{\xi}^s$ is the scattered vector in the elliptic basis. This gives the scattering matrix $S^1 = USU^{-1}$ referred to an elliptic basis.

Suppose the transformation, U, in equation (B18) gives a right-hand elliptically polarised incident electric field, then the transformation given by equation (B20) produces a left-hand elliptically polarised scattered field since the direction of propagation is reversed. This is because when we talk of left- or right-handedness a direction is associated with it and when we speak in this way we are effectively using a different cartesian system for the two directions of propagation - one being right-handed for the incident wave, the other left-handed for the scattered wave as viewed by an observer at large distance (eg, at the radar).

It is convenient to use a different transformation on the scattered field so that in the example above a right-handed elliptically polarised scattered field is produced. We can do this by using

$$\underline{\xi}^s = U * \underline{E}^s, \quad \dots(B21)$$

so that the scattering matrix

$$S^1 = U * S U^{-1} \quad \dots(B22)$$

gives right-hand transmit, right-hand receive and left-hand transmit, left-hand receive on the main diagonals of S^1 . By taking the complex conjugate of U , we have effectively changed the signs of ϕ_x and ϕ_y in equation (B11), thus changing the sense of the polarisation.

B7. FORM OF TRANSFORMATION MATRIX

The unitary condition (B17) has been imposed on U to preserve magnitudes of vectors, so only four of the eight quantities (the four complex u_{ij}) in the transformation are independent. The most general such matrix may be written

$$U^{-1} = \begin{bmatrix} \cos \zeta e^{i\eta_{11}}, & -\sin \zeta e^{i\eta_{12}} \\ \sin \zeta e^{i(\eta_{11} + \eta_{22} - \eta_{12})}, & \cos \zeta e^{i\eta_{22}} \end{bmatrix}. \quad \dots(B23)$$

The determinant of U^{-1} is $e^{i(\eta_{11} + \eta_{22})}$. Thus, the determinant of S is not preserved under the transformation (B22) but has its phase altered. We follow other authors [20-22] in imposing the condition that the determinant of the transformation, U , is unity. The most general such matrix is now

$$U^{-1} = \begin{bmatrix} \cos \zeta e^{i\eta_{11}}, & -\sin \zeta e^{i\eta_{12}} \\ \sin \zeta e^{-i\eta_{12}}, & \cos \zeta e^{-i\eta_{11}} \end{bmatrix}. \quad \dots(B24)$$

This contains three unknowns which may be related to the phase, ellipticity and the orientation of the elliptical vector formed by the transformation [21]. This may be brought out by making the following substitutions:-

$$\tan \eta_{11} = -\tan \psi \tan \alpha,$$

$$\tan \eta_{12} = -\cot \psi \tan \alpha,$$

$$\tan \zeta = \tan^2 \psi \frac{1 + \tan^2 \psi \tan^2 \alpha}{\tan^2 \psi + \tan^2 \alpha}.$$

The transformation matrix [22] now becomes

$$Q = U^{-1} = R(\psi)H(\alpha), \quad \dots(B26)$$

where
$$R(\psi) = \begin{bmatrix} \cos \psi, & -\sin \psi \\ \sin \psi, & \cos \psi \end{bmatrix} \quad \dots(B27)$$

and
$$H(\alpha) = \begin{bmatrix} \cos \alpha, & i \sin \alpha \\ i \sin \alpha, & \cos \alpha \end{bmatrix}. \quad \dots(B28)$$

We shall go on to show that $R(\psi)$ is a rotation matrix that determines the orientation of the major axis of the ellipse and that $H(\alpha)$ is an ellipticity matrix which determines the ratio of major to minor axes. We have reduced the 3 unknowns in equation (B24) to 2 in equation (B26) effectively by choosing an arbitrary phase factor but this does not matter since phase can only be determined to within an arbitrary additive constant. The extra condition we have imposed can be written as

$$\tan \zeta = \frac{\cos \eta_{12}}{\cos \eta_{11}} \sqrt{\tan \eta_{11} \cot \eta_{12}}, \quad \dots(B29)$$

but this appears to have no physical significance.

It is worth noting that the matrices R and H do not commute, ie, $RH \neq HR$. With the transformation matrix given by equation (B26) we see that the determinant of S is preserved under the transformation [22] since $Q^{*T} Q = I$ and $\det Q = 1$ so that

$$\det S^1 = \det (Q^T S Q) = \det Q^T \det S \det Q = \det S. \quad \dots(B30)$$

Also preserved is the trace of the power scattering matrix [2]. This matrix is defined as

$$P = S^{*T} S. \quad \dots(B31)$$

Now
$$\begin{aligned}
P^1 &= S^{1*T} S^1, \\
&= (Q^{*T} S^{*T} Q^*) (Q^T S Q), \\
&= Q^{*T} S^{*T} S Q, \\
&= Q^{*T} P Q.
\end{aligned}
\tag{B32}$$

The trace (ie, the sum of the diagonal elements) represents the total power that would be returned to a pair of orthogonally polarised antennae and is given by

$$\text{Tr}(P) = |S_{11}|^2 + |S_{22}|^2 + |S_{12}|^2 + |S_{21}|^2. \tag{B33}$$

Now
$$\begin{aligned}
\text{Tr}(P^1) &= P_{11} (Q_{11}^* Q_{11} + Q_{12}^* Q_{12}) + P_{12} (Q_{11}^* Q_{21} + Q_{12}^* Q_{22}) \\
&\quad + P_{21} (Q_{21}^* Q_{11} + Q_{22}^* Q_{12}) + P_{22} (Q_{21}^* Q_{21} + Q_{22}^* Q_{22}), \\
&= P_{11} + P_{22}, \\
&= \text{Tr}(P),
\end{aligned}$$

where the P_{ij} and Q_{ij} are the elements of P and Q respectively.

B8. ROTATION MATRIX

For positive ψ the matrix $R(\psi)$ operating on the vector \underline{V} will rotate \underline{V} in the xy plane by an amount ψ in a counter clockwise (left-hand) direction looking along the direction of propagation (see figure B3). Following a rotation the elements of the scattering matrix become:-

$$\begin{aligned}
S_{11}^1 &= S_{11} \cos^2 \psi + (S_{12} + S_{21}) \cos \psi \sin \psi + S_{22} \sin^2 \psi, \\
S_{12}^1 &= (S_{22} - S_{11}) \cos \psi \sin \psi + S_{12} \cos^2 \psi - S_{21} \sin^2 \psi, \\
S_{21}^1 &= (S_{22} - S_{11}) \cos \psi \sin \psi + S_{21} \cos^2 \psi - S_{12} \sin^2 \psi, \\
S_{22}^1 &= S_{11} \sin^2 \psi - (S_{12} + S_{21}) \cos \psi \sin \psi + S_{22} \cos^2 \psi.
\end{aligned}
\tag{B37}$$

Note that these do not agree with reference [22] in which a sign has been changed between their equation (12) and their equation (18).

We see that

$$S_{11}^1 + S_{22}^1 = S_{11} + S_{22},$$

and

$$S_{12}^1 - S_{21}^1 = S_{12} - S_{21}.$$

B9. ELLIPTICITY MATRIX

The matrix $H(\alpha)$ operating on the vector $\begin{pmatrix} 1 \\ 0 \end{pmatrix}$ produces the vector $\begin{pmatrix} \cos \alpha \\ i \sin \alpha \end{pmatrix}$. Using equation (B9) this may be interpreted as an electric field for which $A_x = \cos \alpha$, $A_y = \sin \alpha$ and $\phi_x = 0$, $\phi_y = \pi/2$. The magnitude of the field is (from equation (B12))

$$|\underline{E}| \sqrt{\cos^2 \alpha \cos^2 (\omega t + kz) + \sin^2 \alpha \sin^2 (\omega t + kz)},$$

so that \underline{E} traces out an ellipse with ratio of minor to major axes given by $\tan \alpha$. Provided α is positive, then the circulation, looking in the direction of propagation, is clockwise (or right-handed) as shown in figure B4(a)*. When $\alpha = \pm \pi/4$, we get circular polarisation.

When $H(\alpha)$ operates on $\begin{pmatrix} 0 \\ 1 \end{pmatrix}$ an elliptically polarised field is again produced, the major axis now being at right-angles to that obtained from $H(\alpha)\begin{pmatrix} 1 \\ 0 \end{pmatrix}$ and the circulation direction being of opposite sense, as shown in figure B4(b). Thus, the phase zero of $H(\alpha)\begin{pmatrix} 0 \\ 1 \end{pmatrix}$ leads that of $H(\alpha)\begin{pmatrix} 1 \\ 0 \end{pmatrix}$ by 90° .

Suppose $H(\alpha)$ operates on $\begin{bmatrix} 1 \\ \sqrt{2} \\ 1 \\ \sqrt{2} \end{bmatrix}$, then the vector field obtained is $\begin{bmatrix} \frac{1}{\sqrt{2}} e^{i\alpha} \\ \frac{1}{\sqrt{2}} e^{i\alpha} \end{bmatrix}$ so that $A_x = A_y = \frac{1}{\sqrt{2}}$, $\phi_x = \phi_y = \alpha$. This is a linearly polarised

field (figure B4(c)). This should not be surprising since we have noticed that the rotation and ellipticity matrices do not commute and to obtain

$\begin{bmatrix} 1 \\ \sqrt{2} \\ 1 \\ \sqrt{2} \end{bmatrix}$ from $\begin{pmatrix} 1 \\ 0 \end{pmatrix}$ requires a rotation of 45° . Thus, we shall only get the

elliptic polarisation we are expecting if we operate with $H(\alpha)$ on either $\begin{pmatrix} 1 \\ 0 \end{pmatrix}$ or $\begin{pmatrix} 0 \\ 1 \end{pmatrix}$, ie, before operating with the rotation matrix.

*Note that this does not agree with reference [22] unless their conventions on circulation direction are opposite to ours.

Following a change of ellipticity the scattering matrix elements become:-

$$\begin{aligned}
 S_{11}^1 &= S_{11} \cos^2 \alpha + i(S_{12} + S_{21}) \sin \alpha \cos \alpha - S_{22} \sin^2 \alpha, \\
 S_{12}^1 &= i(S_{11} + S_{22}) \sin \alpha \cos \alpha + S_{12} \cos^2 \alpha - S_{21} \sin^2 \alpha, \\
 S_{21}^1 &= i(S_{11} + S_{22}) \sin \alpha \cos \alpha - S_{12} \sin^2 \alpha + S_{21} \cos^2 \alpha, \\
 S_{22}^1 &= S_{11} \sin^2 \alpha + i(S_{12} + S_{21}) \cos \alpha \sin \alpha + S_{22} \cos^2 \alpha.
 \end{aligned}
 \tag{B36}$$

Note that $S_{11}^1 + S_{22}^1 = (S_{11} + S_{22}) \cos 2\alpha + i(S_{12} + S_{21}) \sin 2\alpha$,

$$S_{11}^1 - S_{22}^1 = S_{11} - S_{22},$$

$$S_{12}^1 - S_{21}^1 = S_{12} - S_{21},$$

and that the phase zero of S_{12}^1 , S_{21}^1 leads S_{11}^1 by 90° while that of S_{22}^1 leads S_{11}^1 by 180° .

For circular polarisation $\alpha = +\pi/4$ for right-hand and $\alpha = -\pi/4$ for left-hand rotation. This gives (for $\alpha = +\pi/4$):-

$$\begin{aligned}
 S_{11}^1(\pi/4) &= \frac{1}{2} (S_{11} - S_{22} + i(S_{12} + S_{21})), \\
 S_{12}^1(\pi/4) &= \frac{1}{2} (i(S_{11} + S_{22}) + S_{12} - S_{21}), \\
 S_{21}^1(\pi/4) &= \frac{1}{2} (i(S_{11} + S_{22}) - S_{12} + S_{21}), \\
 S_{22}^1(\pi/4) &= \frac{1}{2} (-S_{11} + S_{22} + i(S_{12} + S_{21})).
 \end{aligned}
 \tag{B37}$$

We may change the notation slightly to make this more meaningful. By remembering our conventions, we have for right-hand transmit and right-hand receive $S_{11}^1(\pi/4)$ which we re-write as C_{RR} where the first suffix refers to the receiver and the second suffix to the transmitter. Similarly for transmit in the direction of increasing θ and receive in the direction of increasing θ we have S_{11} which we re-write as $S_{\theta\theta}$. In this way equation (B37) may be re-written as:-

$$\begin{aligned}
C_{RR} &= \frac{1}{2} (-S_{\phi\phi} + S_{\theta\theta} + i(S_{\phi\theta} + S_{\theta\phi})), \\
C_{RL} &= \frac{1}{2} (i(S_{\phi\phi} + S_{\theta\theta}) - S_{\phi\theta} + S_{\theta\phi}), \\
C_{LR} &= \frac{1}{2} (i(S_{\phi\phi} + S_{\theta\theta}) + S_{\phi\theta} - S_{\theta\phi}), \\
C_{LL} &= \frac{1}{2} (+S_{\phi\phi} - S_{\theta\theta} + i(S_{\phi\theta} + S_{\theta\phi})),
\end{aligned}
\tag{B38}$$

where again the first suffix refers to the receiver and the second to the transmitter. The phase zero of C_{RL} and C_{LR} leads that of C_{RR} by 90° while that of C_{LL} leads that of C_{RR} by 180° .

B10. COMBINED EFFECT OF ROTATION AND ELLIPTICITY CHANGE

Since the rotation matrix and the ellipticity matrix do not commute, the transformation (B35) must be performed first followed by equation (B36). The expressions for the elements of the new scattering matrix in terms of the original are not particularly informative and so are not given explicitly. However, for the special case of circular polarisation we have:-

$$\begin{aligned}
C_{RR}^1 &= C_{RR} e^{-2i\psi}, \\
C_{LL}^1 &= C_{LL} e^{2i\psi}, \\
C_{LR}^1 &= C_{LR}, \\
C_{RL}^1 &= C_{RL}.
\end{aligned}
\tag{B39}$$

Despite the differences noted earlier, reference [22] agrees with these formulae.

We now define four radar cross-sections invariant under rotations and these are:-

$$I = 4\pi r^2 \{ |C_{RR}|^2 + |C_{LL}|^2 + |C_{RL}|^2 + |C_{LR}|^2 \},$$

$$J = 4\pi r^2 |C_{LR}|^2,$$

$$K = 4\pi r^2 |C_{RR}|^2,$$

$$L = 4\pi r^2 |C_{LL}|^2,$$

....(B40)

assuming the incident plane wave has unit modulus. Here r is, as before, the distance from the scatterer to the receiver. Note that

$$I = 4\pi r^2 \{ |S_{\theta\theta}|^2 + |S_{\phi\phi}|^2 + |S_{\phi\theta}|^2 + |S_{\theta\phi}|^2 \} \quad \text{....(B41)}$$

also, and that for a monostatic radar (ie, one for which the transmitter and the receiver are in the same place)

$$I = 2J + K + L. \quad \text{....(B42)}$$

For a body of revolution, with the coordinate axis along the body axis, we have in the monostatic case [23]

$$S_{\theta\phi} = 0, \quad S_{\phi\theta} = 0 \quad \text{....(B43)}$$

and for arbitrary rotation ψ of the polarisation axes:-

$$\begin{aligned} C_{RR}^1 &= \frac{1}{2} (S_{\theta\theta} - S_{\phi\phi}) e^{-2i\psi}, \\ C_{LL}^1 &= -\frac{1}{2} (S_{\theta\theta} - S_{\phi\phi}) e^{2i\psi}, \\ C_{LR}^1 &= C_{RL}^1 = \frac{1}{2} i(S_{\theta\theta} + S_{\phi\phi}), \end{aligned} \quad \text{....(B44)}$$

and

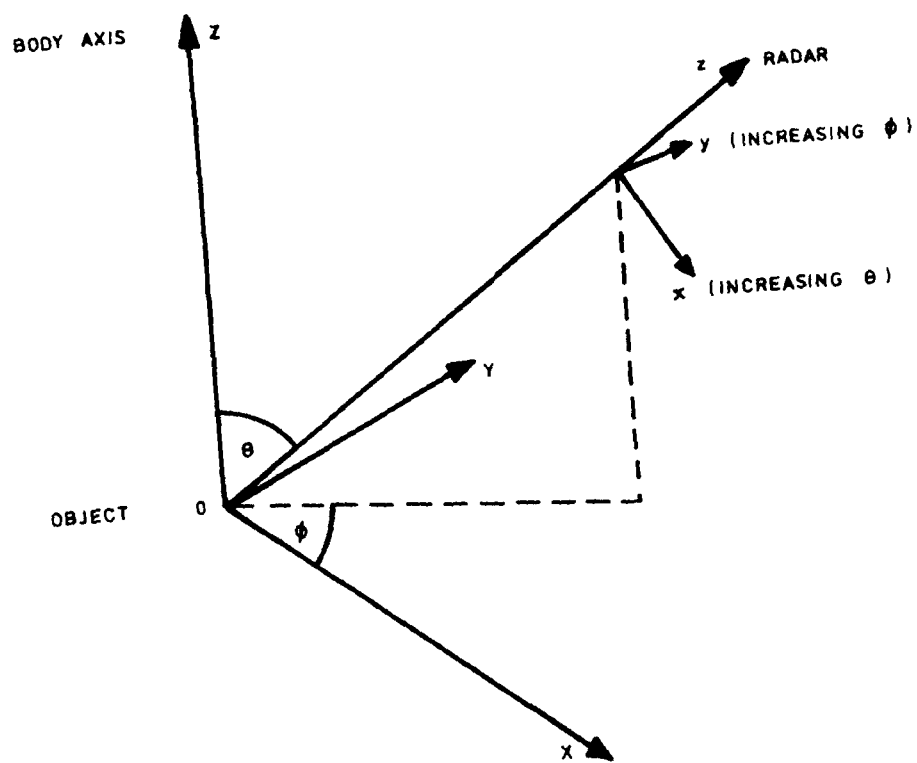
$$\begin{aligned} S_{\theta\theta}^1 &= S_{\theta\theta} \cos^2 \psi + S_{\phi\phi} \sin^2 \psi, \\ S_{\theta\phi}^1 &= S_{\phi\theta}^1 = (S_{\phi\phi} - S_{\theta\theta}) \cos \psi \sin \psi, \\ S_{\phi\phi}^1 &= S_{\theta\theta} \sin^2 \psi + S_{\phi\phi} \cos^2 \psi. \end{aligned} \quad \text{....(B45)}$$

B11. DEPOLARISATION

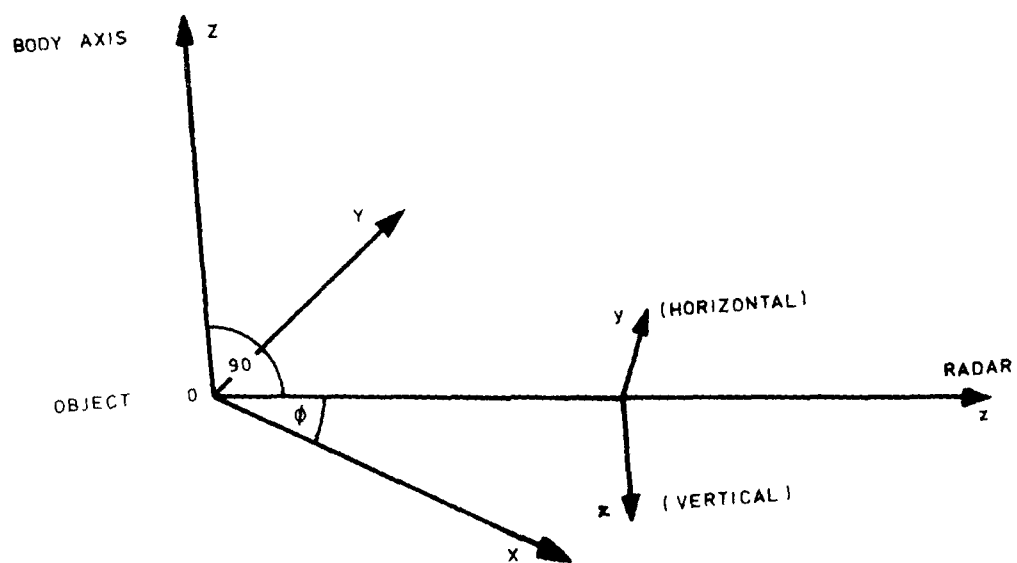
Bickel [22] defines a quantity D_n , which he calls the depolarisation, as

$$\begin{aligned}
 D_n &= 1 - \frac{|S_{\theta\theta} + S_{\phi\phi}|^2}{2\text{Tr}(P)}, \\
 &= \frac{\frac{1}{2} |S_{\theta\theta} - S_{\phi\phi}|^2 + |S_{\theta\phi}|^2 + |S_{\phi\theta}|^2}{|S_{\theta\theta}|^2 + |S_{\theta\phi}|^2 + |S_{\phi\theta}|^2 + |S_{\phi\phi}|^2}, \quad \dots(B46) \\
 &= \frac{|C_{LL}|^2 + |C_{RR}|^2}{|C_{LL}|^2 + |C_{LR}|^2 + |C_{RL}|^2 + |C_{RR}|^2}.
 \end{aligned}$$

A sphere, for which C_{LL} and C_{RR} are zero, has $D_n = 0$ while a dipole, for which $S_{\theta\phi} = S_{\phi\theta} = S_{\phi\phi} = 0$, say, has $D_n = \frac{1}{2}$. Bickel then goes on to show that larger values of D_n characterize bodies with multiple scattering centres. D_n is invariant to rotations but not to ellipticity changes. D_n is calculated by CHAOS automatically but its usefulness has not yet been assessed.

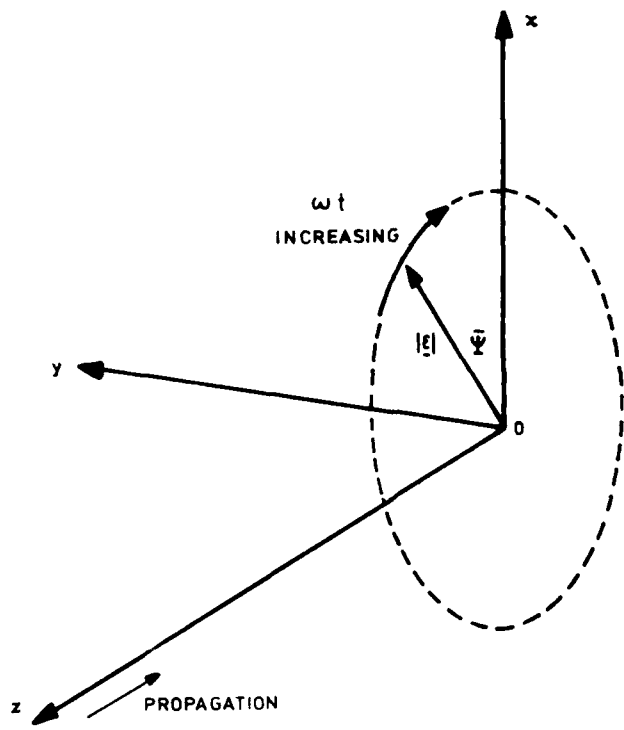


B1 (a) General Case

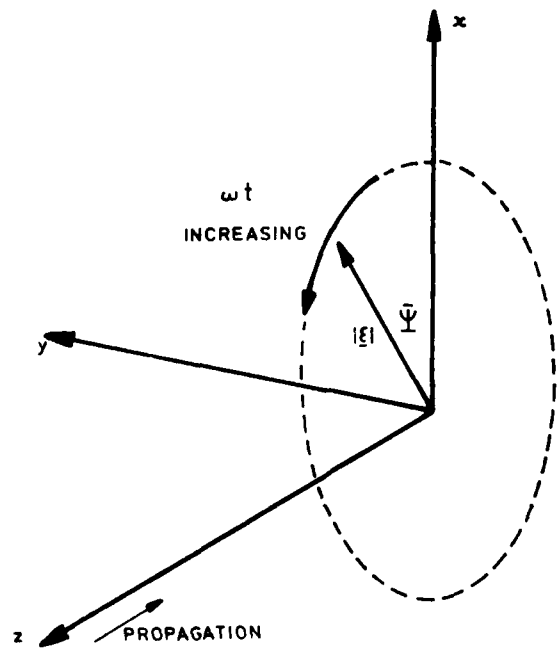


B1 (b) Special Case

FIGURE B1 Co-ordinate Systems



CLOCKWISE
(RIGHT HAND)
ROTATION



ANTI CLOCKWISE
(LEFT HAND)
ROTATION

FIGURE B2 Elliptic Polarisation

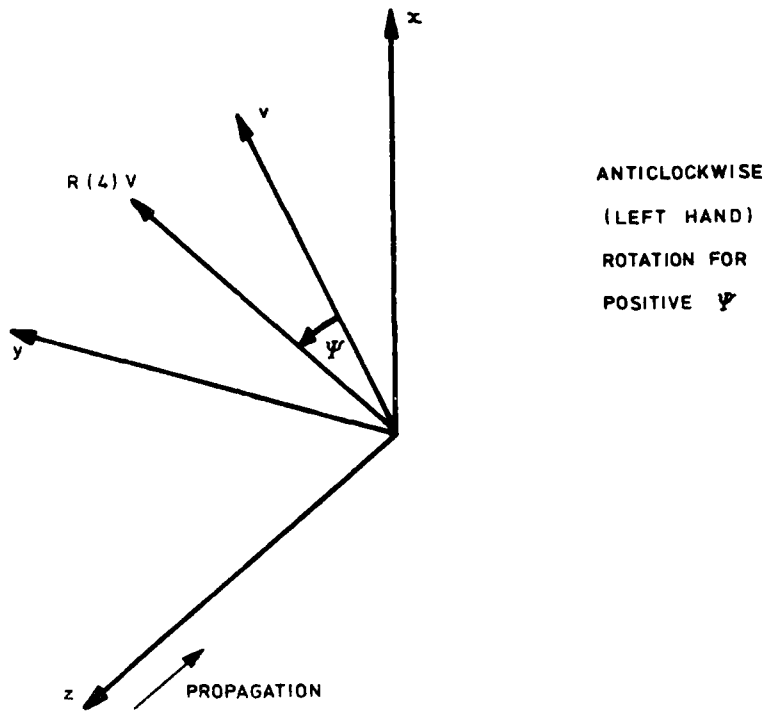
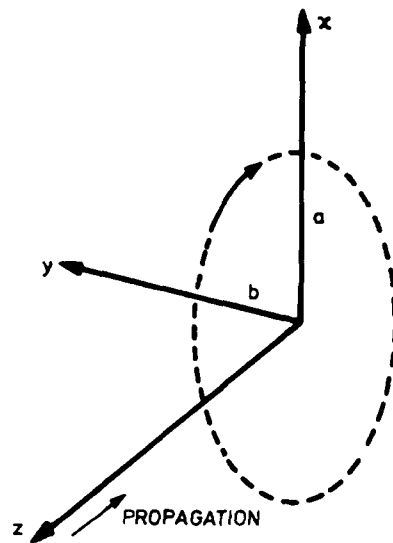


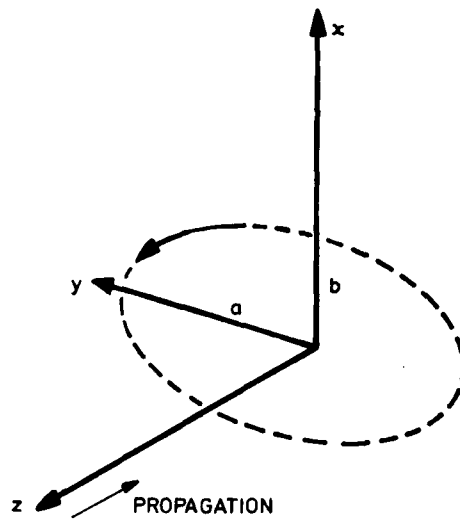
FIGURE B3 Effect of Rotation Matrix



$$\tan \alpha = b/a > 0$$

CLOCKWISE
(RIGHT HANDED)
ELLIPTIC
POLARISATION

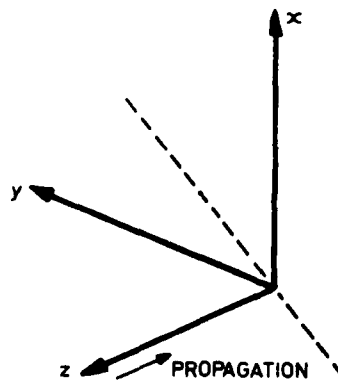
B4 (a) $H(\alpha) \begin{pmatrix} 1 \\ 0 \end{pmatrix}$



$$\tan \alpha = b/a > 0$$

ANTICLOCKWISE
(LEFT HANDED)
ELLIPTIC
POLARISATION

B4 (b) $H(\alpha) \begin{pmatrix} 0 \\ 1 \end{pmatrix}$



LINEAR
POLARISATION

B4 (c) $H(\alpha) \begin{pmatrix} 1/\sqrt{2} \\ 1/\sqrt{2} \end{pmatrix}$

FIGURE B4 Effect of Ellipticity Matrix

APPENDIX C

LIST OF SYMBOLS

Many of these symbols, when used in the text, have suffices or superfixes associated with them. Not all of these are separately defined here. This list is not complete but covers the most frequently used symbols.

C1. COORDINATE SYSTEMS AND GEOMETRY

OXYZ		object coordinate system
Oxyz		radar coordinate system
$\underline{r} = (x, y, z)$		general coordinate vector
t		time
a		wire radius
l		length along wire
θ, ϕ		spherical polar coordinates in OXYZ system
$\underline{u}_x, \underline{u}_y$		unit vectors in Ox and Oy directions
$R = \underline{r} - \underline{r}' $	=	distance between observation point, \underline{r} , and some source point, \underline{r}'
ds	=	element of surface area
\underline{n}	=	unit normal to surface
d ℓ	=	element of wire length
$\underline{T}(\ell)$	=	triangle function
\underline{u}	=	unit vector
D_{jm}^{in}	=	scalar product between vectors in directions $\underline{r}_{jm+1} - \underline{r}_{jm}$ and $\underline{r}_{in+1} - \underline{r}_{in}$ where \underline{r}_{jm} is the vector from the origin to the start of segment m under triangle function \underline{T}_j
Δ	=	segment length

C2.

ELECTRIC FIELDS

$\underline{\mathcal{E}}(\underline{r}, t)$	= real electric field
$\underline{E}(\underline{r}, t)$	= complex electric field
$\underline{E}(\underline{r})$	= complex electric field assuming $e^{i\omega t}$ time variation
\underline{D}	= complex electric flux
\underline{H}	= complex magnetic field
\underline{B}	= complex magnetic flux
\underline{J}	= complex conduction current
$\underline{I}(\ell)$	= complex line density of current
ρ	= complex electric charge
$\sigma(\ell)$	= complex line density of charge
ϵ	= dielectric constant
μ	= magnetic permeability
σ	= conductivity
$c = \frac{1}{\sqrt{\epsilon\mu}}$	= velocity of light in medium
ν	= frequency in cycles/sec
$\omega = 2\pi\nu$	= frequency in radians/sec
$\eta = c\mu = \frac{1}{c\epsilon} = \sqrt{\frac{\mu}{\epsilon}}$	= impedance of medium
$\lambda = \frac{2\pi c}{\omega} = \frac{c}{\nu}$	= wavelength
$k = 2\pi/\lambda = \frac{\omega}{c}$	= wave number
$T = \sqrt{-i\omega\mu(\sigma+i\omega\epsilon)}$	= complex wave number
\underline{A}	= magnetic vector potential
ϕ	= electric scalar potential
A_j	= magnitude of $\underline{\mathcal{E}}_j$, $j = x, y, z$
ϕ_j	= phase of $\underline{\mathcal{E}}_j$, $j = x, y, z$
ψ	= angle between $\underline{\mathcal{E}}_j(\underline{x}, t)$ and the x axis
$\underline{\xi}$	= complex electric field intensity referred to an elliptic polarisation basis
\underline{V}	= voltage vector
Z_ω	= impedance of wire

Z	= impedance matrix
$g(\theta, \phi)$	= radar cross-section in direction (θ, ϕ)
P	= power
ψ	= integral defined by equation (49) or (A1)
δ	= skin depth
η	= loss angle
R, L, C	= resistance, inductance and capacitance

C3. SCATTERING MATRICES

S	scattering matrix, elements S_{ij}
$P = S^{*T} S$	power scattering matrix, elements P_{ij}
U	unitary transformation matrix
$\zeta, \eta_{11}, \eta_{12}, \eta_{22}$	the four independent quantities in the unitary matrix U
α	ellipticity angle (arctan of ratio of minor to major axes of ellipse)
ψ	rotation angle (of body about radar line of sight)
$R(\psi)$	rotation matrix
$H(\alpha)$	ellipticity matrix
$Q = U^{-1} = R(\psi)H(\alpha)$, elements Q_{ij}	
$S_{\theta\theta}, S_{\theta\phi}, S_{\phi\theta}, S_{\phi\phi}$	are the elements of the scattering matrix S referred to linearly polarised fields in the directions of increasing θ or ϕ . The first suffix referring to the receiver, the second to the transmitter
$C_{RR}, C_{RL}, C_{LR}, C_{LL}$	are the elements of the scattering matrix S referred to circularly polarised fields with right, R, or left, L, hand circulation

$$I = 4\pi r^2 \{ |C_{RR}|^2 + |C_{RL}|^2 + |C_{LR}|^2 + |C_{LL}|^2$$

$$J = 4\pi r^2 |C_{LR}|^2 \quad \text{the sphere accept radar cross-section}$$

$$K = 4\pi r^2 |C_{RR}|^2 \quad \text{a sphere reject radar cross-section}$$

$$L = 4\pi r^2 |C_{LL}|^2 \quad \text{another sphere reject radar cross-section}$$

$$D_n \quad \text{depolarisation.}$$

REFERENCES

- 1(a) H H Chao and B J Strait: "Computer Programs for Radiation and Scattering by Arbitrary Configurations of Bent Wires". AFCRL-70-0374, Scientific Report Number 7 on Contract No. F19628-68-C-0180 (September 1970)
- 1(b) M D Tew: "Correction to WIRES Program". IEEE, AP23, 450 (1975)
2. J R Mautz and R F Harrington: "Computer Programs for Characteristic Modes of Wire Objects". AFCRL-71-0174, Scientific Report Number 11 on Contract No. F19628-68-C-0180 (March 1971)
3. D C Kuo and B J Strait: "Improved Programs for Analysis of Radiation and Scattering by Configurations of Arbitrarily Bent Thin Wires". AFCRL-72-0051, Scientific Report Number 15 on Contract No. F19628-68-C-0180 NAPS 01798 (January 1972)
4. J H Richmond: "Computer Program for Thin Wire Structures in a Homogeneous Conducting Medium". National Technical Information Service, Springfield, Va 22151, NASA Contractor Report CR-2399 (June 1974)
5. Harwell Subroutine Library, a Catalogue of Subroutines (1973). Supplement No. 2. Compiled by M J Hopper. AERE R-7477, Supplement No. 2
6. R Fletcher: "Factorizing Symmetric Indefinite Matrices". Linear Algebra and its Applications, 14, 257 (1976)
7. S Marlow and J K Reid: "Fortran Subroutines for the Solution of Linear Equations, Inversion of Matrices and Evaluation of Determinants". AERE R-6899 (September 1971)
8. R F Harrington: "Matrix Methods for Field Problems". Proc IEEE, 55, 136 (1967)
9. J L Lin, W L Curtis and M C Vincent: "Radar Cross-Section of a Rectangular Conducting Plate by Wire Mesh Modelling". IEEE, AP22, 718 (1974)
10. E P Sayre: "Junction Discontinuities in Wire Antenna and Scattering Problems". IEEE, AP21, 216 (1973)
- 11(a) C M Butler, R M Duff, R W P King and E Yung: "Theoretical and Experiment Investigations of Thin Wire Structures, Junction Conditions, Currents and Charges". AFWL Interaction Note 238 (February 1975)
- 11(b) T T Wu and R W P King: "The Tapered Antenna and Its Application to the Junction Problem for Thin Wires". IEEE, AP24, 42 (1976)

12. M Abramowitz and I A Stegun: "Handbook of Mathematical Functions". p363, National Bureau of Standards (1965)
13. I S Duff: "MA28 - A Set of FORTRAN Subroutines for Sparse Unsymmetric Linear Equations". AERE R-8730 (July 1977)
14. F M Tesche: "On the Analysis of Scattering and Antenna Problems Using the Singularity Expansion Technique". IEEE Trans, AP21, 53 (1973)
15. S D Conte and C de Boor: "Elementary Numerical Analysis". McGraw Hill, pp74-83 (1972)
16. B K Singaraju, D V Giri and C E Baum: "Further Developments in the Application of Contour Integration to the Evaluation of the Zeroes of Analytic Functions and Relevant Computer Programs". Air Force Weapons Laboratory, Kirtland Air Force Base, New Mexico, USA, Mathematics Notes, Note Number 42 (March 1976)
17. G T Ruck (Editor): "Radar Cross-Section Handbook". Plenum Press (1970)
18. "IRE Standards on Radio Wave Propagation". Supplement to Proc IRE, 30, 2 (1942)
19. "Methods of Radar Cross Section Analysis". Edited by J W Crispin and K M Siegel, Academic Press (1968)
20. V H Rumsey: "Part I: Transmission Between Elliptically Polarised Antennas". Proc IRE, 39, 535 (1951)
21. C D Graves: "Radar Polarisation Power Scattering Matrix". Proc IRE, 44, 248 (1956)
22. S H Bickel: "Properties of the Polarisation Scattering Matrix". Proc IEEE, 53, 1070 (1965)
23. M G Andreasen: "Scattering from Bodies of Revolution". IEEE Trans, AP13, 303 (1965)

REPRINTS OF FIELD ARTICLES NECESSARILY
 AVAILABLE TO MEMBERS OF THE PUBLIC
 OR TO COMMERCIAL ORGANISATIONS

DOCUMENT CONTROL SHEET

Overall security classification of sheet UNCLASSIFIED

(As far as possible this sheet should contain only unclassified information. If it is necessary to enter classified information, the box concerned must be marked to indicate the classification eg (R), (C) or (S)).

1. DRIC Reference (if known) -	2. Originator's Reference AWRE Report No. 044/79	3. Agency Reference -	4. Report Security Classification UNLIMITED
5. Originator's Code (if known) -	6. Originator (Corporate Author) Name and Location Atomic Weapons Research Establishment, Aldermaston, Berkshire		
5a. Sponsoring Agency's Code (if known) -	6a. Sponsoring Agency (Contract Authority) Name and Location -		
7. Title The Calculation of Radar Cross-Sections			
7a. Title in Foreign Language (in the case of Translation) -			
7b. Presented at (for Conference Papers). Title, Place and Date of Conference -			
8. Author 1.Surname, Initials Pizer R	9a. Author 2 -	9b. Authors 3, 4 -	10. Date ² pp ref February 1980 91 23
11. Contract Number -	12. Period -	13. Project -	14. Other References -
15. Distribution Statement RESTRICTED			
16. Descriptors (or Keywords) (TEST) Computer programs CHAOS FORTRAN Radar cross sections			
Abstract This report provides a detailed description of the methods used in the computer program CHAOS for calculating radar cross-sections.			

Some Metric and SI Unit Conversion Factors

(Based on DEF STAN 00-11/2 "Metric Units for Use by the Ministry of Defence",
DS Met 5501 "AWRE Metric Guide" and other British Standards)

Quantity	Unit	Symbol	Conversion
<u>Basic Units</u>			
Length	metre	m	1 m = 3.2808 ft 1 ft = 0.3048 m
Mass	kilogram	kg	1 kg = 2.2046 lb 1 lb = 0.45359237 kg 1 ton = 1016.05 kg
<u>Derived Units</u>			
Force	newton	$N = \text{kg m/s}^2$	1 N = 0.2248 lbf 1 lbf = 4.44822 N
Work, Energy, Quantity of Heat	joule	$J = \text{N m}$	1 J = 0.737562 ft lbf 1 J = 9.47817×10^{-4} Btu 1 J = 2.38846×10^{-4} kcal 1 ft lbf = 1.35582 J 1 Btu = 1055.06 J 1 kcal = 4186.8 J 1 W = 0.238846 cal/s 1 cal/s = 4.1868 W
Power	watt	$W = J/s$	
Electric Charge	coulomb	$C = A s$	-
Electric Potential	volt	$V = W/A = J/C$	-
Electrical Capacitance	farad	$F = A s/V = C/V$	-
Electric Resistance	ohm	$\Omega = V/A$	-
Conductance	siemen	$S = 1 \Omega^{-1}$	-
Magnetic Flux	weber	$Wb = V s$	-
Magnetic Flux Density	tesla	$T = Wb/m^2$	-
Inductance	henry	$H = V s/A = Wb/A$	-
<u>Complex Derived Units</u>			
Angular Velocity	radian per second	rad/s	1 rad/s = 0.159155 rev/s 1 rev/s = 6.28319 rad/s
Acceleration	metre per square second	m/s^2	1 m/s^2 = 3.28084 ft/s^2 1 ft/s^2 = 0.3048 m/s^2
Angular Acceleration	radian per square second	rad/s^2	-
Pressure	newton per square metre	$N/m^2 = Pa$	1 N/m^2 = 145.038×10^{-6} lbf/in ² 1 lbf/in ² = 6.89476×10^3 N/m^2
	bar	$bar = 10^5 N/m^2$	-
Torque	newton metre	N m	1 in. Hg = 3386.39 N/m^2 1 N m = 0.737562 lbf ft 1 lbf ft = 1.35582 N m
Surface Tension	newton per metre	N/m	1 N/m = 0.0685 lbf/ft 1 lbf/ft = 14.5939 N/m
Dynamic Viscosity	newton second per square metre	$N s/m^2$	1 $N s/m^2$ = 0.0208854 lbf s/ft ² 1 lbf s/ft ² = 47.8803 $N s/m^2$
Kinematic Viscosity	square metre per second	m^2/s	1 m^2/s = 10.7639 ft^2/s 1 ft^2/s = 0.0929 m^2/s
Thermal Conductivity	watt per metre kelvin	W/m K	-
<u>Odd Units*</u>			
Radioactivity	becquerel	Bq	1 Bq = 2.7027×10^{-11} Ci 1 Ci = 3.700×10^{10} Bq
Absorbed Dose	gray	Gy	1 Gy = 100 rad 1 rad = 0.01 Gy
Dose Equivalent	sievert	Sv	1 Sv = 100 rem 1 rem = 0.01 Sv
Exposure	coulomb per kilogram	C/kg	1 C/kg = 3876 R 1 R = 2.58×10^{-4} C/kg
Rate of Leak (Vacuum Systems)	millibar litre per second	mb l/s	1 mb = 0.750062 torr 1 torr = 1.33322 mb

*These terms are recognised terms within the metric system.

DATE
ILMED
— 88